

DRAFT

**CIRCULATION MODELING FOR THE
PROPOSED PORT FACILITY AT
PONCE AND GUAYANILLA, PUERTO RICO**

By

Norman W. Scheffner, Fulton C. Carson, and David J. Mark
Coastal and Hydraulics Laboratory

DEPARTMENT OF THE ARMY
U.S. Army Engineer Research and Development Center
Waterways Experiment Station
Coastal and Hydraulics Laboratory
3909 Halls Ferry Road, Vicksburg, Mississippi 39180-6199

17 September 2001

Prepared for

US Army Engineer District, Jacksonville
400 West Bay Street
P.O. Box 4970
Jacksonville, Florida 32232-0019

Abstract

This report documents a tidal and storm surge circulation study conducted by the U.S. Army Engineer Waterways Experiment Station's Coastal and Hydraulics Laboratory to evaluate the protection provided by the proposed construction of a deep-draft harbor facility in the ports of Ponce and Guaynilla, Puerto Rico. Impacts of the proposed construction were determined by conducting numerical simulations of tidal and storm surge circulation at the project sites using with and without the proposed port facilities. Differences in computed elevations and currents between pre- and post-construction conditions are used to determine impacts. Numerical simulations utilize the long-wave hydrodynamic model ADCIRC.

Conclusions of this study are twofold. First, simulations show that the harbors of Ponce and Guayanilla do not experience large tides or tropical and extratropical storm surges. Secondly, pre- and post-project simulations of a severe tropical event show that project impacts are small (less than 1.0 m/sec) and that localized reductions in storm circulation currents which do not affect regions further than approximately 1 km from the proposed project sites.

Introduction

The Jacksonville District of the U.S. Army Corps of Engineers requested assistance from the Coastal and Hydraulics Laboratory of the Waterways Experiment Station of the U.S. Army's Engineer Research and Development Center, Vicksburg Mississippi, in evaluating circulation impacts of the proposed mega-port facility at Ponce and Guayanilla Harbors along the southern coast of Puerto Rico. The approach taken to access circulation impacts utilizes the long-wave hydrodynamic model ADCIRC to compute circulation patterns with and without the projects. Impacts are then quantified by computing magnitude changes at the two harbors. Impacts will be shown for tidal circulation as well as for tropical and extratropical storm surge. The following sections briefly describe: 1) the ADCIRC hydrodynamic model, 2) verification of the ADCIRC model, 3) storm event boundary conditions, 4) project impact, and 5) conclusions.

1. The Hydrodynamic Model

In the following two sub-sections, documentation for the hydrodynamic model is first given to provide a background of model development and demonstrate the applicability of the ADCIRC model to represent the study area. This section is followed by a description of the computational grid developed for the Puerto Rico study.

Model Documentation

Water-surface elevations and currents for both tides and storm events are computed through applications of the large-domain long-wave hydrodynamic Advanced CIRCulation (ADCIRC) model (Luettich, Westerink, and Scheffner 1992). The ADCIRC model is an unstructured grid finite-element long-wave model developed under the U.S. Army Corps of Engineers (USACE) Dredging Research Program (DRP, Griffis et al 1995). The model was developed as a family of two- and three-dimensional codes with the capability of:

- a. Simulating tidal circulation and storm surge propagation over large computational domains while simultaneously providing high resolution in areas of complex shoreline and bathymetry. The targeted areas of interest include continental shelves, nearshore areas, and estuaries.
- b. Representing all pertinent physics of the three-dimensional equations of motion. These include tidal potential, Coriolis, and all nonlinear terms of the governing equations.
- c. Providing accurate and efficient computations over time periods ranging from months to years.

In two dimensions, model formulation begins with the depth-averaged shallow-water equations for conservation of mass and momentum subject to incompressibility and hydrostatic pressure approximations. The Boussinesq approximation, where density is considered constant in all terms but the gravity term of the momentum equation, is also incorporated in the model. Using the standard quadratic parameterization for bottom stress and omitting baroclinic terms and lateral diffusion and dispersion, the following set of

conservation statements in primitive, non-conservative form and expressed in a spherical coordinate system are incorporated in the model (Flather 1988; Kolar et al. 1994):

$$\frac{\partial \zeta}{\partial t} + \frac{1}{R \cos \phi} \left[\frac{\partial UH}{\partial \lambda} + \frac{\partial(UV \cos \phi)}{\partial \phi} \right] = 0 \quad (1)$$

$$\begin{aligned} \frac{\partial U}{\partial t} + \frac{1}{r \cos \phi} U \frac{\partial U}{\partial \lambda} + \frac{1}{R} V \frac{\partial U}{\partial \phi} - \left[\frac{\tan \phi}{R} U + f \right] V = \\ - \frac{1}{R \cos \phi} \frac{\partial}{\partial \lambda} \left[\frac{P_s}{\rho_0} + g(\zeta - \eta) \right] + \frac{\tau_{s\lambda}}{\rho_0 H} - \tau_* U \end{aligned} \quad (2)$$

$$\begin{aligned} \frac{\partial V}{\partial t} + \frac{1}{r \cos \phi} U \frac{\partial V}{\partial \lambda} + \frac{1}{R} V \frac{\partial V}{\partial \phi} - \left[\frac{\tan \phi}{R} U + f \right] U = \\ - \frac{1}{R \cos \phi} \frac{\partial}{\partial \phi} \left[\frac{P_s}{\rho_0} + g(\zeta - \eta) \right] + \frac{\tau_{s\lambda}}{\rho_0 H} - \tau_* V \end{aligned} \quad (3)$$

where t represents time, λ and ϕ are degrees longitude (east of Greenwich is taken positive) and degrees latitude (north of the equator is taken positive), η is the free-surface elevation relative to the geoid, U and V are the depth-averaged horizontal velocities, R is the radius of the Earth, $H = \zeta + h$ is the total water column depth, h is the bathymetric depth relative to the geoid, $f = 2\Omega \sin \phi$ is the Coriolis parameter, Ω is the angular speed of the Earth, p_s is the atmospheric pressure at the free surface, g is the acceleration due to gravity, η is the effective Newtonian equilibrium tide potential, ρ_0 is the reference density of water, $\tau_{s\lambda}$ and $\tau_{s\phi}$ are the applied free-surface stress, and τ_* is given by the expression $C_f(U^2 + V^2)^{1/2} / H$ where C_f equals the bottom friction coefficient which can be specified as either linear or nonlinear (Luettich, Westerink, and Scheffner 1992).

The momentum equations (Equations 2 and 3) are differentiated with respect to λ and t and substituted into the time differentiated continuity equation (Equation 1) to develop the following Generalized Wave Continuity Equation (GWCE):

$$\begin{aligned}
& \frac{\partial^2 \zeta}{\partial t^2} + \tau_0 \frac{\partial \zeta}{\partial t} - \frac{1}{R \cos \phi} \frac{\partial}{\partial \lambda} \left[\frac{1}{R \cos \phi} \left(\frac{\partial(HUU)}{\partial \lambda} + \frac{\partial(HUV \cos \phi)}{\partial \phi} \right) - UVH \frac{\tan \phi}{R} \right] \\
& \left[-2\omega \sin \phi HV + \frac{H}{R \cos \phi} \frac{\partial}{\partial \lambda} \left(g(\zeta - \alpha \eta) + \frac{P_s}{\rho_0} \right) + \tau_* HU - \tau_0 HU - \frac{\tau_{s\lambda}}{\rho_0} \right] \\
& - \frac{1}{R} \frac{\partial}{\partial \phi} \left[\frac{1}{R \cos \phi} \left(\frac{\partial(HVV)}{\partial \lambda} + \frac{\partial(HVV \cos \phi)}{\partial \phi} \right) + UUH \frac{\tan \phi}{R} + 2\omega \sin \phi HU \right] \\
& - \frac{1}{R} \frac{\partial}{\partial \phi} \left[\frac{H}{R} \frac{\partial}{\partial \phi} \left(g(\zeta - \alpha \eta) + \frac{P_s}{\rho_0} \right) + (\tau_* - \tau_0) HV - \frac{\tau_{s\phi}}{\rho_0} \right] \\
& - \frac{\partial}{\partial t} \left[\frac{VH}{R} \tan \phi \right] - \tau_0 \left[\frac{VH}{R} \tan \phi \right] = 0
\end{aligned} \tag{4}$$

The ADCIRC-2DDI model solves the GWCE (Equation 4) in conjunction with the primitive momentum equations given in Equations 2 and 3.

The ADCIRC model solves the governing equations with a finite-element algorithm over arbitrary bathymetry encompassed by irregular sea and shore boundaries. This algorithm allows for flexible spatial discretizations over the entire computational domain and has demonstrated robust stability characteristics. The advantage of this flexibility in developing a computational grid is that larger elements can be specified in open-ocean regions where less resolution is needed, whereas smaller elements can be applied in nearshore and estuarine areas where finer resolution is required to resolve hydrodynamic details.

The Computational Grid

The ADCIRC model has been applied to the east coast, Gulf of Mexico, and Caribbean Sea domain shown in Figure 1 to develop a tidal constituent data base (Westerink et al 1993). This grid was used as a basis for the present Puerto Rico circulation study. A sub-section of the grid of Figure 1 was first developed in which the southern boundary was maintained at the coasts of Venezuela and Columbia, the western boundary placed mid-way through the island of Hispaniola, and the northern boundary defined as an arc extending north from Hispaniola and eastward. The eastern boundary was then defined by extending the arc eastward of the Lesser Antilles to intersect with the open coast of Surinam. The grid and boundaries for the present study are shown in Figure 2. Bathymetry for the domain was initially provided from the National Imagery and Mapping Agency (NIMA 2000) digital data base of bathymetry.

Figure 1 The DRP east coast, Gulf of Mexico, Caribbean Sea grid

Figure 2 Computational domain of the Puerto Rico study

Resolution of the grid in the study areas was increased to provide a minimum grid spacing of approximately 30 m. This resolution allows for accurate representation of the

proposed deep-draft navigation channel and docking facility at Ponce and Guayanilla.. The increased resolution provided for the harbors is shown in Figures 3a and 3b. Existing Bathymetry shown for Ponce was extracted from the NIMA digital nautical chart for North America West. Existing bathymetry for Guayanilla was not included in the NIMA data base and was manually entered based on NOS nautical chart 25681.

Figure 3a Grid resolution and existing bathymetry at Ponce

Figure 3b Grid resolution and existing bathymetry at Guayanilla

2. Verification of the ADCIRC Model

Verification of the model is required to assure that grid resolution, bathymetry, and boundary conditions are adequately prescribed to acceptably reproduce known or observed events. Because storm surge data are not available for the study area, verification is limited to reproduction of tidal surface elevations at locations within the modeled domain shown in Figure 2 for which tidal constituent data are readily available.

Tidal propagation is simulated within ADCIRC by specifying a surface elevation time series at each of the open-water nodes of the computational grid of Figure 2. These time series are based on the digital tidal constituent data base of Le Provost et al (1994) for the M_2 , S_2 , N_2 , K_1 , O_1 , P_1 , Q_1 , and K_2 tidal constituents. The Le Provost data base has been successfully used in all recent CHL tidal studies requiring tidal boundary conditions because of its comprehensive coverage of the world and its consistent accuracy in open water. The ADCIRC model was run with these boundary conditions for a 15 day simulation period. Computed surface elevation time series were archived at various locations in the computational domain for comparison to a surface elevation time series reconstructed from existing harmonic analyses.

Existing harmonic constituent data were available for 15 stations within the study domain from the National Oceanic and Atmospheric Administration's (NOAA) National Ocean Survey (NOS) and the International Hydrographic Organization (IHO 1991). Station locations are listed in Table 1 and shown in Figure 4.

Table 1 Station locations

Station Number	East Longitude (degs)	North Latatude (degs)	Station Name
1	-66.1167	18.4617	San Juan, La Puntilla, San Juan Bay, PR
2	-64.7533	17.6967	Lime Tree Bay, St Croix, USVI
3	-64.8700	18.3200	Benner Bay, St Thomas, USVI
4	-64.9200	18.3350	Charlotte Amalie, St Thomas, USVI
5	-68.9333	12.1000	Willemstad, Curacao
6	-66.9333	10.6167	La Guaira, Venezuela
7	-64.1667	10.4500	Cumana, Venezuela
8	-61.5167	10.6500	Port of Spain, Trinidad
9	-61.0000	14.0167	Castries, St. Lucia
10	-61.0500	14.5833	Fort-de-France, Martinique
11	-64.9333	18.3333	St. Thomas, U.S. Virgin Islands
12	-67.0500	17.9667	Magueyes Island, Puerto Rico
13	-69.8833	18.4667	Ciudad, Trujillo, Dominican Republic
14	-70.6833	19.7500	Puerto Plato, Dominican Republic
15	-64.8833	16.5333	IAPSO #30-1.3.2

Figure 4 Station locations within model domain

Because harmonic data are not available at Ponce and Guayanilla, verification was limited to demonstrating that the model acceptably reproduces tidal elevations throughout the modeled domain. Therefore, verification is limited to a visual comparison of model simulated time series versus reconstructed time series based on published harmonic constituents. Figures 5 and 6 show comparisons of simulated and reconstructed data for the Puerto Rico coastal stations of San Juan (Station 1) and Magueyes Island (Station 12). The full set of comparisons are shown in Appendix A. As shown in the figures, the simulation provides sufficient accuracy to satisfy the goals of the present study, therefore, it is concluded that the model and associated grid are verified for tides. Because tides and surges are both examples of long waves, the conclusion that the model is verified to tides translates into the assumption that the model can acceptably reproduce tropical and extratropical storm surge.

Figure 5 Comparison of ADCIRC and IHO/NOS reconstructed tide at San Juan

Figure 6 Comparison of ADCIRC and IHO/NOS reconstructed tide at Magueyes Island

3. Storm event boundary conditions

The basis of determining project impacts to the study area of interest was determined to be magnitude differences in surface elevations and current magnitudes as a result of the proposed project. This difference was to be defined for both tidal circulation and tropical and extratropical storm surge. Tidal boundary conditions are based on the

tidal constituent-based boundary conditions used in verification. Storm surges were selected as historic events that impacted the island of Puerto Rico. The following two sub-sections describe the selection of storm events to be used in the storm surge comparison.

Tropical storm surge

The hurricane wind field model used in conjunction with the ADCIRC model is the Hurricane Planetary Boundary Layer (PBL) model developed by Cardone (Cardone, Greenwood, and Greenwood 1992). This model simulates hurricane-generated wind and atmospheric pressure fields by solving the equations of horizontal motion which have been vertically averaged through the depth of the planetary boundary layer. The PBL model input consists of “histogram” and “snapshot” files which define the hourly location in latitude and longitude of the eye of the storm and the storm intensity parameters specified at defined times.

Snapshot and histogram files are computed from data contained in the National Oceanic and Atmospheric Administration’s (NOAA) National Hurricane Center's HURricane DATAbase (HURDAT) of tropical storm events (Jarvinen, Neumann, and Davis 1988). This database contains descriptions of all hurricane, tropical storm and severe tropical depressions which have impacted the east coast, Gulf of Mexico, and Caribbean Sea from 1886 to present.

A tropical storm database was generated during the DRP (Scheffner, et al 1994) through simulation of 134 historically based storm events along the east coast, Gulf of Mexico, and Caribbean Sea based on the HURDAT data base. For 486 discrete locations along the U.S. coast, peak storm surge values corresponding to storm events which produced a surge of at least 0.305 m. were archived and indexed according to event, location, and surge magnitude. This indexed database, as well as the most current version of the HURDAT data, were used to select Hurricane Georges, which crossed Puerto Rico on 22 September 1998, as the event for determining hurricane impact to the study area. A plot of the track of Hurricane Georges is shown in Figure 7.

Figure 7 Track of Hurricane Georges

Extratropical storm surge

In an approach similar to that of the tropical event database described above, an extratropical storm event database was generated within the DRP. This database was constructed by driving the ADCIRC model with wind fields extracted from the U.S. Navy Fleet Numerical Meteorology and Oceanography Center's database of winds for the 16-year winter storm period (defined as September through March) of 1977 through 1993 (77-78, 78-79, etc). These windfield data are provided at a 6-hour temporal interval on a 2.5° latitude and longitude spatial grid. The extratropical storm database consists of a 7-month surface elevation and current hydrograph at each of the 486 stations described above.

Time series plots corresponding to an archived station near the center of the study area were analyzed for peak values in surface elevation and current magnitude. Each time series represented surge with no tide. The time series plot corresponding to DRP Station 682, located offshore of Ponce and Guayanilla, was generated for each of the 16 storm year periods. One period of extratropical surge was found to occur during the extratropical storm year 1992-1993 shown in Figure 8. In this figure, day 1 refers to 1 September 1982 such that the storm event of day 195 refers to 15 March 1993.

Figure 8 Surge values for extratropical storm year 1992-1993 at DRP station 682

4. Project Impact

Project impacts were defined to be changes in surface elevation and/or depth-averaged currents as a result of the construction of the proposed harbor facilities. In the following two sections, the specifics of both proposed projects are summarized. This summary is followed by results of the numerical simulations for with and without project construction. For each project scenario, contours of maximum surface elevation and maximum current magnitude and vector differences are used to quantify project impacts.

Ponce Harbor

The proposed deep-draft harbor complex at Ponce Harbor involves the deepening of the navigation channel to a minimum of 13.7 m and development of a new dock facility in the harbor. This new dockage will require the reclaiming of approximately 60 acres of water to the immediate north of Punta Penoncillo. The area of reclaimed water is shown in the project footprint superimposed on the topographical map in Figure 9. The model representation of the reclaimed feature is shown in Figure 10. It is assumed that the reclaimed area is not subject to wetting and drying but will remain a permanent land feature. Minimum depths in the navigation channel are set to 15.0 m.

Figure 9 Topographic map of Ponce with project footprint

Figure 10 Model representation of proposed Ponce Harbor

Guayanilla Harbor

The proposed deep-draft harbor complex in Guayanilla Harbor involves construction of an extensive harbor facility on land fill just north of the end of Punta Guayanilla as shown in Figure 11. The offloading facility adjoining the land fill will be on piers and not represent an obstruction of flow. Model representation of the reclaimed feature is shown in Figure 12. It is assumed that the reclaimed area is a permanent land feature and not subject to wetting and drying. The offloading pier is located in deep water such that no dredging is required.

Figure 11 Topographic map of Guayanilla with project footprint

Figure 12 Model representation of proposed Guayanilla Harbor

Simulation results - Tides

Harbor construction impact on tidal circulation was based on an analysis of a 28-day tidal month simulation over the full domain. The tide was based on the 8 constituents used in model verification and did not include winds. Resulting time series of tidal elevations and currents were archived at the 15 reference locations shown in Figures 13 for Ponce and Guayanilla.

Figure 13 Reference stations for the Ponce and Guayanilla Harbors

Tides along the southern coast of Puerto Rico are primarily diurnal with one high tide per day as shown in the time series for Magueyes Island in Figure 6. Because all reference stations are in unprotected open water and the two harbors are adjacent to each other, reference station tides are essentially identical. For example, the 28-day surface elevation time series for Stations 8 and 13 are shown in 14. Note in the figure that the first 2 days show a reduced amplitude due to starting the model from Mean Sea Level (MSL) and ramping the tide to full amplitude in 3 days. Therefore tides representative of the study area should be taken from days 3-28. The tidal current magnitude is shown in Figure 15 for the corresponding 28 days.

Figure 14 28-day tidal elevation pre-construction time series for Station 8 and 13

Figure 15 28-day tidal current magnitude pre-construction time series for Station 8 and 13

Tides in both Ponce and Guayanilla Harbors are small with a maximum spring tide amplitude on the order of 0.15 m and currents less than 1cm/sec. However, in order to quantify construction impacts over the entire harbor area, time series of surface elevation and currents are archived at all computational nodes of the model to facilitate generation of maximum magnitude difference contour maps and difference vector maps. Although tides are not much affected by local changes to the shoreline configuration or bottom bathymetry, the impact of the two harbor projects are shown in Figure 15 for tidal surface elevation extreme (maximum or minimum) differences and Figure 16 for maximum tidal current magnitude vector differences. The time period for computed maximum differences was selected as the spring tide period of days 12.5 through 17.5 of Figure 14. In Figure 15, differences represent the maximum elevation before construction less the maximum elevation after construction of the landfills (i.e., the maximum difference occurring during the 5-day spring tide of figure 14). Similarly, the vectors and vector magnitudes shown in Figure 16 represent the pre-construction current vector less the post construction vector at the time of greatest difference. Therefore, the magnitude of the vector represents the reduction or increase in currents as a result of construction of the proposed harbor facilities.

Figure 16 Maximum tidal elevations differences during days 12.5-17.5

Figure 17 Maximum tidal current differences during days 12.5-17.5

Figure 18 Maximum tidal current differences during days 12.5-17.5

Inspection of Figures 16-18 shows the proposed harbors generate minimal impact on tidal circulation. For example, maximum elevation changes at either Ponce or Guayanilla are less than 0.01 cm with corresponding current magnitude differences of less than 1.0 cm/sec. These small impacts are to be expected however do to the slow change of tide for the diurnal signal and the fact that wind forcing is not included in the tidal simulations. Wind impacts are addressed below in the tropical storm event simulation of Hurricane Georges.

Simulation results - Tropical

Impacts of the proposed projects can best be evaluated by looking at extreme events. For this reason, Hurricane Georges was selected as the test tropical event. Hurricane Georges passed over the Island of Puerto Rico on 22 September 1998 generating a positive storm surge in both Ponce and Guayanilla Harbors due to the wind-forcing of water into the harbors from the southwest quadrant of the storm as it passed north of the study areas. Storm surge elevations at open water Stations 8 and 13 are shown in Figure 19.

Figure 19 Storm surge elevation for Hurricane Georges at Stations 8 and 13

Storm surges in the Caribbean Sea are generally small as shown in the surge values of Figure 19. This is due to the fact that surges in the Caribbean propagate from deep water immediately into shallow water with no broad continental shelf to force shoaling. Therefore, large surges characteristic of the east and Gulf coasts of the United States do not occur in the Caribbean Sea.. However, wind driven circulation can be significant in shallow harbors and protected areas, therefore, circulation impacts of the proposed projects are used to evaluate project impact.

Figures 20 and 21 show wind driven circulation vectors in Ponce Harbor with and without the proposed harbor expansion computed at the time of the peak of the storm (day 3.28 of Figure 19). Similarly, Figures 22 and 23 show circulation vectors in Guayanilla Harbor with and without the proposed expansion. Figures 20-24 also indicate surface elevation contours that show maximum surge elevations of less than 0.4 m. Figures 24 and 25 show maximum current difference vectors computed during the life of the event superimposed on maximum current magnitude difference contours for Ponce and Guayanilla Harbors. Figures 23 and 24 demonstrate maximum impacts of the proposed harbors and indicate current reductions to be on the order of up to 1.0 m/sec. Maximum reductions are shown to be at Guayanilla Harbor where the pre-construction surge circulation vectors of Figure 21 are shown to be deflected offshore in Figure 22. However, impacts of the proposed harbor expansion are limited to the close proximity of the project.

Figure 20 Pre-expansion circulation vectors at Ponce for Hurricane Georges at day 3.28

Figure 21 Post-expansion circulation vectors at Ponce for Hurricane Georges at day 3.28

Figure 22 Pre-expansion circulation vectors at Guayanilla for Hurricane Georges at day 3.28

Figure 23 Post-expansion circulation vectors at Guayanilla for Hurricane Georges at day 3.28

Figure 24 Maximum current difference at Ponce for Hurricane Georges

Figure 25 Maximum current difference at Guayanilla for Hurricane Georges

Simulation results – Extratropical

The extratropical event of March 1993 described above was selected to represent a winter storm event impact to Ponce and Guayanilla Harbors. Because extratropical event winds are much less intense than tropical events, the resulting surge is found to be considerably smaller than for a tropical event. For example, Figure 26 shown the surface elevations for pre-construction existing conditions at Stations 8 and 13 for the 10 days of simulation (10-20 March 1993). As shown, the surge elevations are less than 10 cm. The corresponding wind driven currents near the proposed harbors at Ponce and Guayanilla were each on the order of 0.2 m/sec as shown in figures 27 and 28 for day 8.125 of Figure 26.

Figure 26 Extratropical storm surge elevation at Stations 8 and 13

Figure 27 Existing condition extratropical storm circulation vectors at Ponce at day 8.125

Figure 28 Existing condition extratropical storm circulation vectors at Guayanilla at day 8.125

Computed maximum differences in current magnitudes and vectors for Ponce and Guayanilla are shown in Figures 29 and 30 to be less than 0.20 m/sec. Currents and current vector differences between pre-and post-construction for the extratropical event are much less than the corresponding computations for the tropical event, therefore, it is concluded that maximum impacts resulting from construction of the proposed harbor complex should be based on the tropical event simulations. Conclusions based on this analysis are presented below.

Figure 29 Maximum extratropical current difference at Ponce

Figure 30 Maximum extratropical current difference at Guayanilla

5. Conclusions

The Coastal and Hydraulics Laboratory of the Waterways Experiment Station was requested by the Jacksonville District of the U.S. Army Corps of Engineers to determine how proposed deep-draft facility expansions of the harbors of Ponce and Guayanilla along the south coast of Puerto Rico may impact the hydrodynamics of the surrounding coastal environment. The ADCIRC long wave hydrodynamic model was used to estimate tidal propagation and storm surge in each of the harbors for both pre-construction existing conditions and post-construction future condition deep-draft harbors. Impacts of the proposed harbor expansions were determined by computing surface elevation and current differences between pre-and post-construction. Events selected for simulation were a typical 28-day lunar month, Hurricane Georges, and an extratropical event of March 1993.

Both Ponce and Guayanilla Harbors have southern exposure that is partially protected by offshore islands and shallow regions. Offshore bathymetry drops to over 600 m within 5-10 km of the entrance to either harbor. Because of the exposure and lack of an offshore shelf, tides and storm surges do not become well develop but remain small. For example, spring tides (without wind) in either harbor are less than 0.2 m in amplitude and the maximum storm surge for Hurricane Georges was less than 0.4 m. Therefore, surface elevation impacts of the proposed harbors are small. For example, the maximum project impact on surface elevation for Hurricane Georges at Guayanilla Harbor was less than 0.05m.

Wind driven currents within the bay represents the most potential long wave threat to the coastal infrastructure resulting from the passage of a tropical or extratropical event. For this reason, change in hurricane surge currents as a result of construction of the harbor expansions was identified as the best measure of construction impact. Pre- and post-construction differences in current magnitudes were computed as a means of demonstrating reductions or increases in current as a result of the proposed landfill.

Computations indicate that pre-construction depth-averaged currents in the vicinity of the Ponce landfill were on the order of 0.5 m/sec during peak positive surge. For Guayanilla Harbor, peak currents at peak surge were also on the order of 0.75 m/sec. Computed maximum differences in current at any time during the storm, i.e., peak positive surge to peak drawdown, were 0.6 - 0.7 m/sec at Ponce and 0.9 - 1.0 m/sec at Guayanilla. The values represent decreases in velocity as a result of the harbor expansions because the constructed landfill deflectes the current offshore of the landfill. These reductions were shown to be very localized such that other regions within the harbor were unaffected by the construction.

Conclusions of this study are twofold. First, simulations show that the harbors of Ponce and Guayanilla do not experience large tides or tropical and extratropical storm surges. Secondly, pre- and post-project simulations of a severe tropical events show that projects impacts are small (less than 1.0 m/sec) localized reductions in storm circulation currents which do not affect regions further than approximately 1 km from the proposed projects.

6. References

Cardone, V.J., Greenwood, C.V., and Greenwood, J.A., (1992). "Unified Program for the Specification of Hurricane Boundary Layer Winds Over Surfaces of Specified Roughness," contract Report CERC-92-1, U.S. Army Engineer Waterways Experiment Station, Vicksburg, MS.

Flather, R. A. (1988). "A numerical model investigation of tides and diurnal-period continental shelf waves along Vancouver Island," *Journal of Physical Oceanography* 18,115-139.

Griffis, F.H., Jettmar, Charles E., Pagdadis, Sotiris, and Tillman, Russel K., 1995, "Dredging Research Program Benefit Analysis," Technical Report DRP-95-8, September 1995, U.S. Army Engineer Waterways Experiment Station, Vicksburg MS.

International Hydrographic Organization Tidal Constituent Bank, 1991, "Station Catalogue," Ocean and Aquatic Sciences, Department of Fisheries and Oceans, Ottawa.

Jarvinen, B.R., Neumann, C.J., and Davis, M.A.S., (1988). "A Tropical Cyclone Data Tape for the North Atlantic Basin, 1886-1983: Contents, Limitations, and Uses," NOAA Technical Memorandum NWS NHC 22.

Kolar, R. L., Gray, W. G., Westerink, J. J., and Luettich, R. A. (1994). "Shallow water modeling in spherical coordinates: Equation formulation, numerical implementation, and application," *Journal of Hydraulic Research* 32(1), 3-24.

Luettich, R.A., Westerink, J.J., and Scheffner, N.W., (1992). "ADCIRC: An Advanced Three-Dimensional Circulation Model for Shelves, Coasts, and Estuaries Report 1: Theory and Methodology of ADCIRC-2DDI and ADCIRC-3DL", Technical Report DRP-92-6, November 1992, U.S. Army Engineer Waterways Experiment Station, Vicksburg MS.

Le Provost, C., Genco, M.L., Lyard, F., Vincent, P., and Canceill, P. (1994). "Spectroscopy of the world ocean tides from a hydrodynamic finite element model," *Journal of Geophysical Research* 99(C12):24,777-24,797.

NIMA, (2000), "National Imagery and Mapping Agency," Digital Nautical Chart, North America West, U.S. Government.

Scheffner, N.W., Mark, D.J., Blain, C.A., Westerink, J.J., and Luetlich, R.A., (1994). "ADCIRC: An Advanced Three-Dimensional Circulation Model for Shelves, Coasts and Estuaries Report 5: A Tropical Storm Data Base for the East and Gulf of Mexico Coasts of the United States," Technical Report DRP-92-6, August 1994, U.S. Army Engineer Waterways Experiment Station, Vicksburg, MS.

Westerink, J.J., Luetlich, R.A., and Scheffner, N.W., (1993), "ADCIRC: An Advanced Three-Dimensional Circulation Model for Shelves, Coasts and Estuaries Report 3: Development of a Tidal Constituent Database for the Western North Atlantic and Gulf of Mexico," Technical Report DRP-92-6, June 1993, U.S. Army Engineer Waterways Experiment Station, Vicksburg, MS.

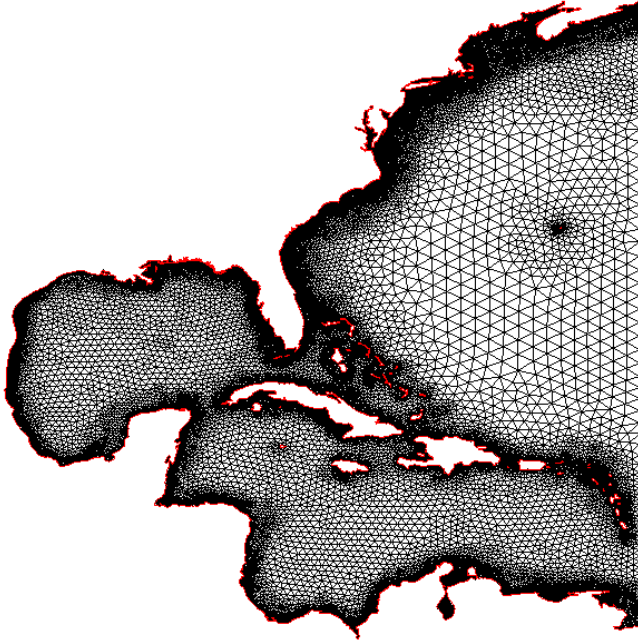


Figure 1 The DRP east coast, Gulf of Mexico, Caribbean Sea grid

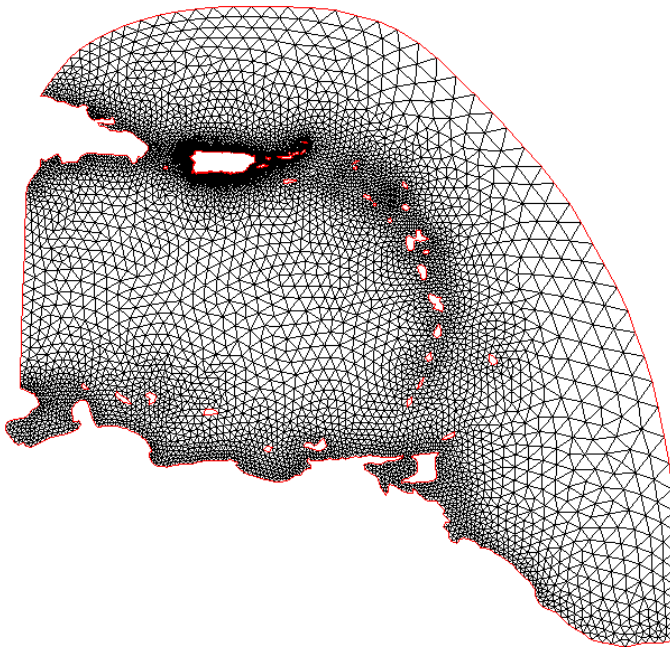


Figure 2 Computational domain of Puerto Rico study

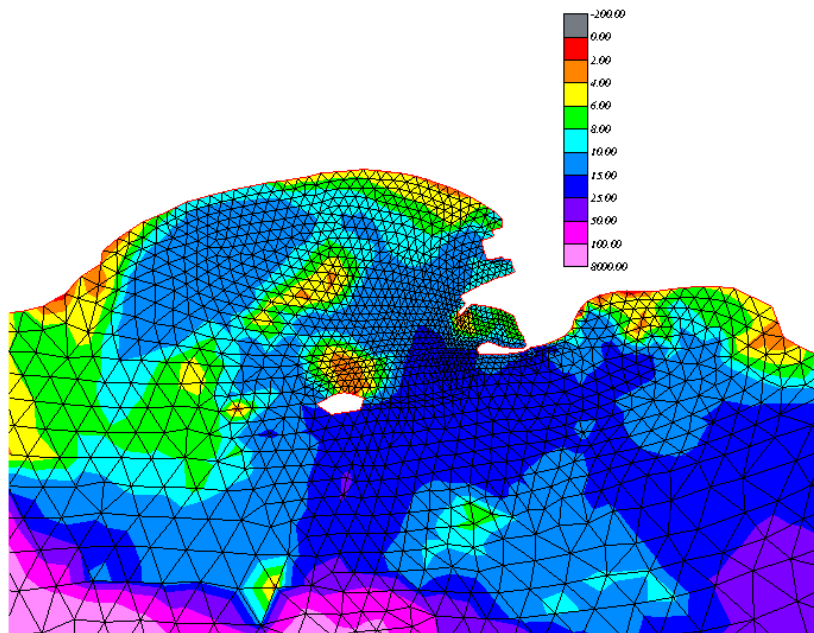


Figure 3a Grid resolution and existing bathymetry at Ponce

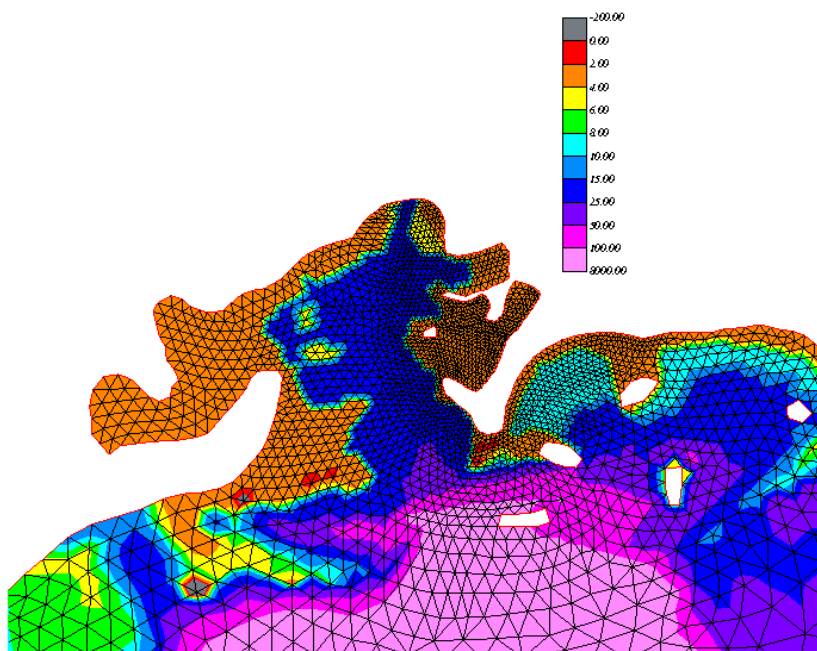


Figure 3b Grid resolution and existing bathymetry at Guayanilla



Figure 4 Station locations within model domain

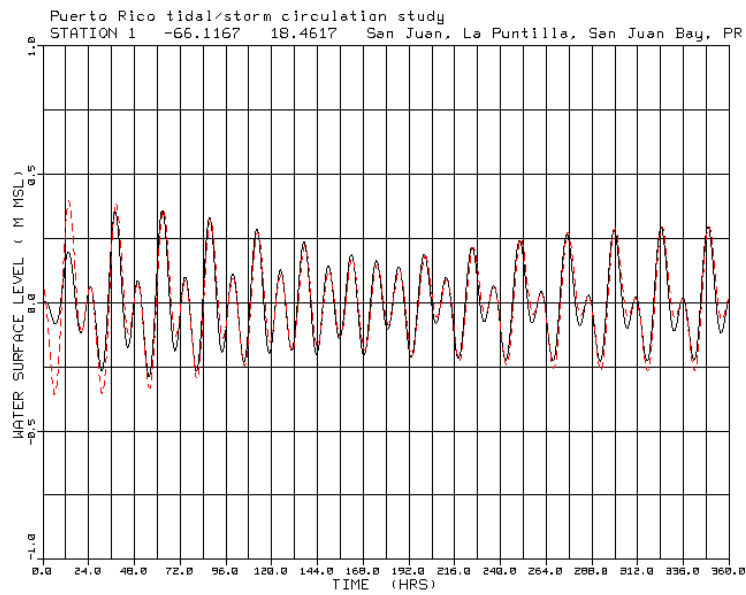


Figure 5 Comparison of ADCIRC and IHO/NOS reconstructed tide at San Juan (Station 1)

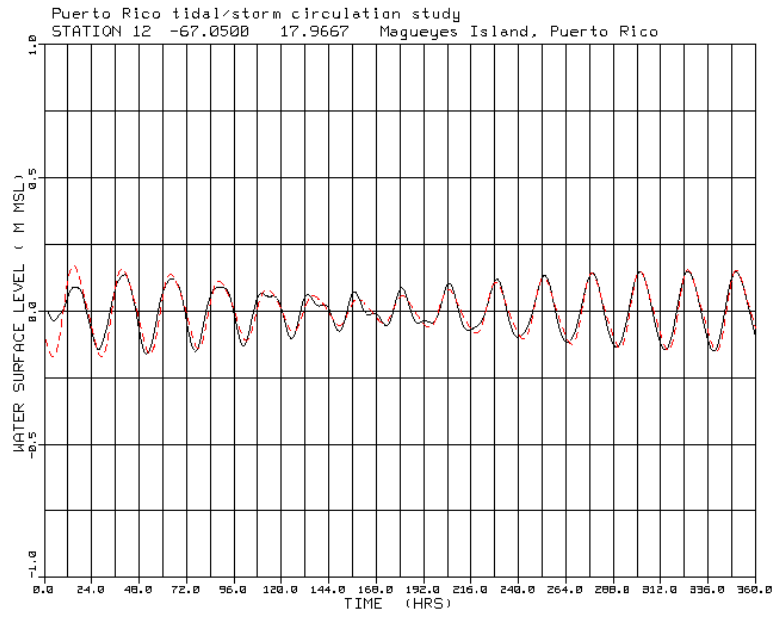


Figure 6 Comparison of ADCIRC and IHO/NOS reconstructed tide at Magueyes Island (Station 12)

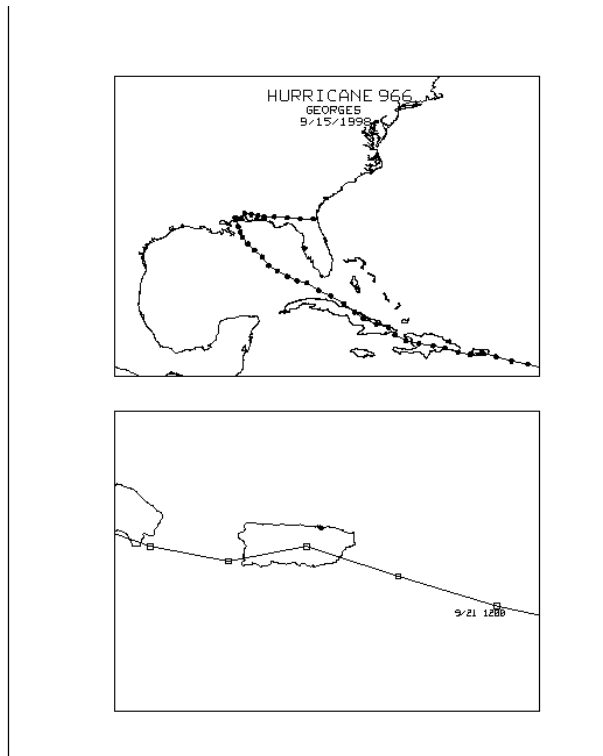


Figure 7 Track of Hurricane Georges

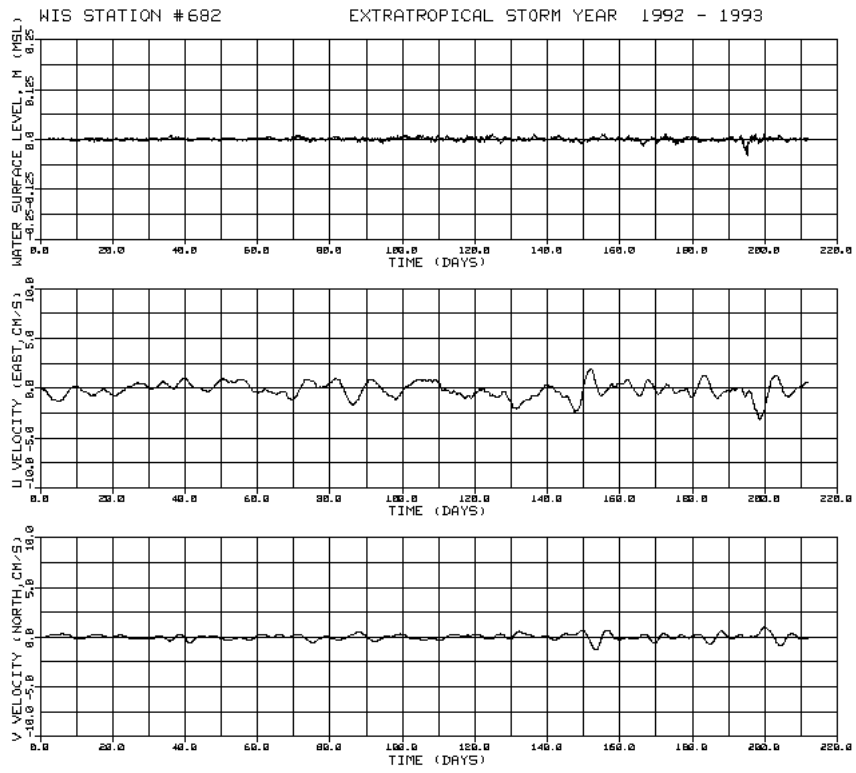


Figure 8 Surge values for extratropical storm year 1992-1993 at DRP station 682

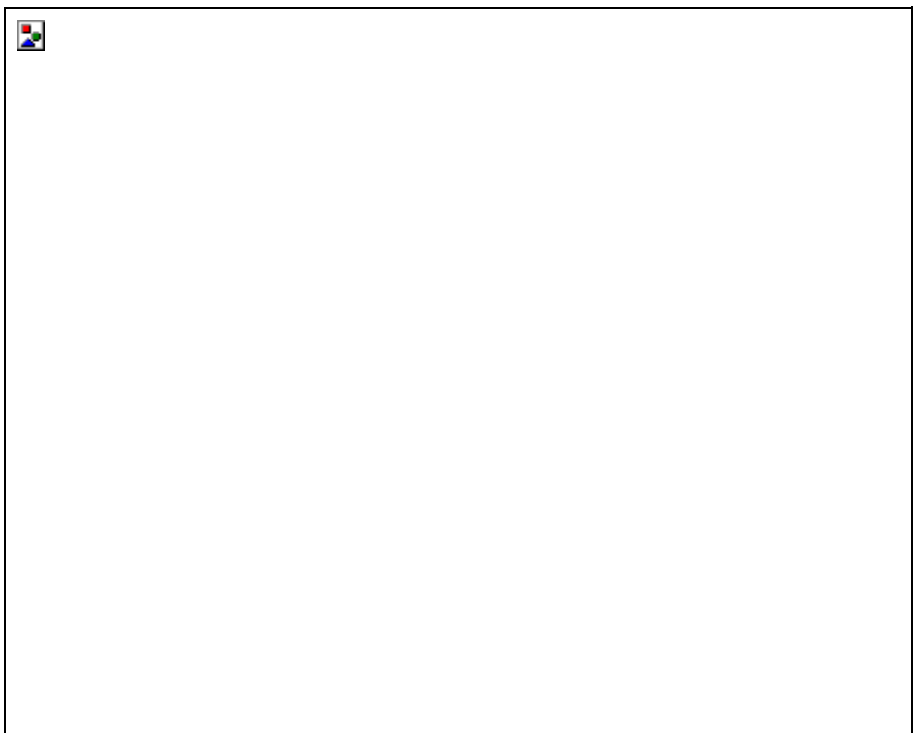


Figure 9 Topographic map of Ponce with project footprint

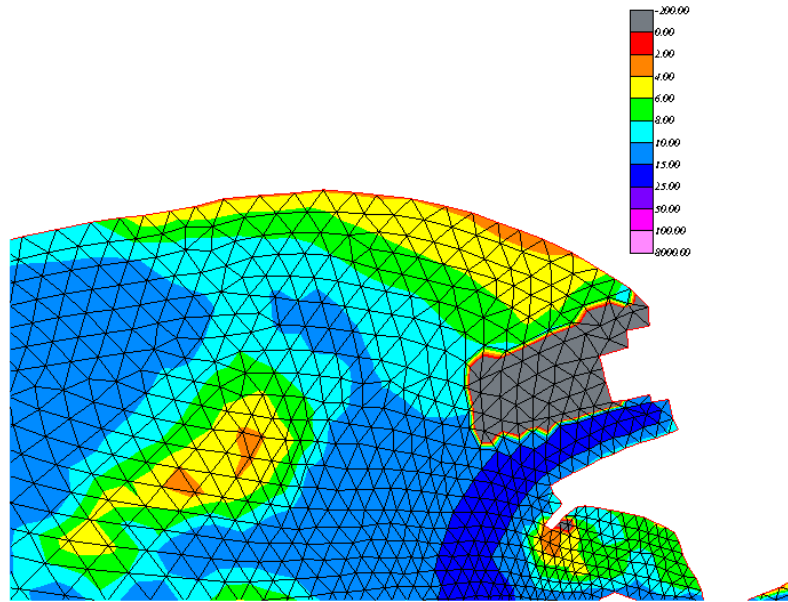


Figure 10 Model representation of proposed Ponce Harbor

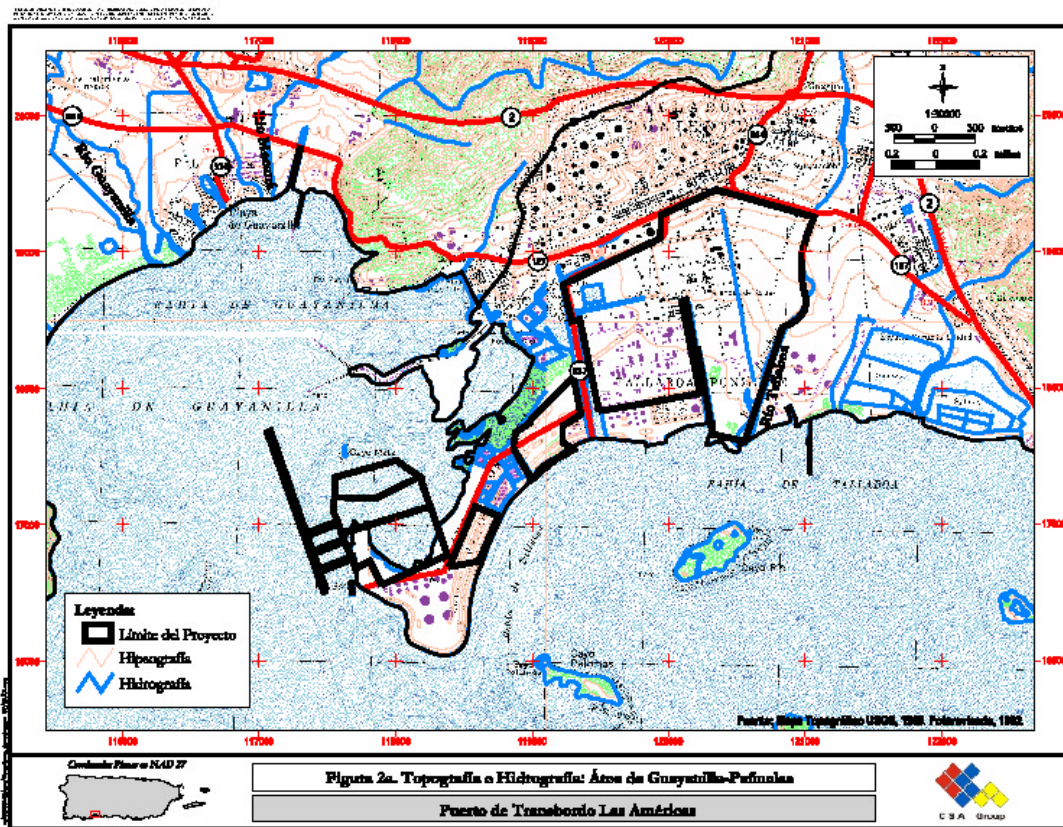


Figure 11 Topographic map of Guayanilla with project footprint

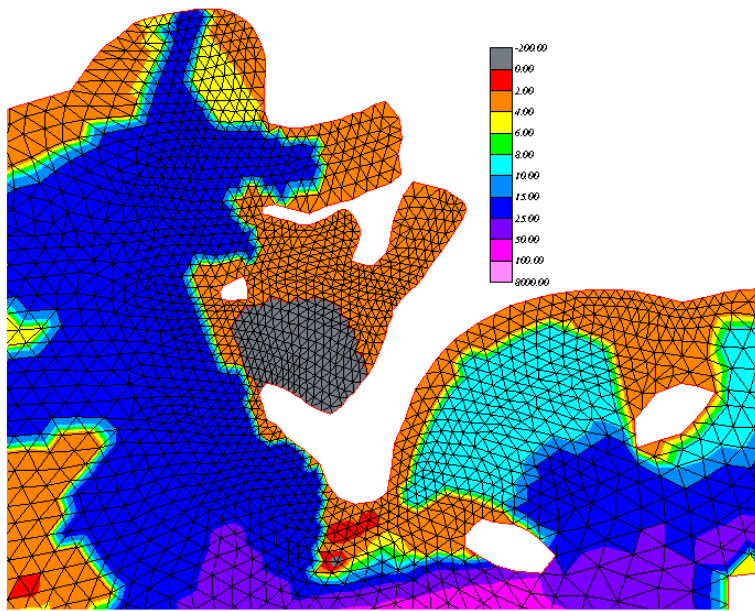


Figure 12 Model representation of proposed Guayanilla Harbor

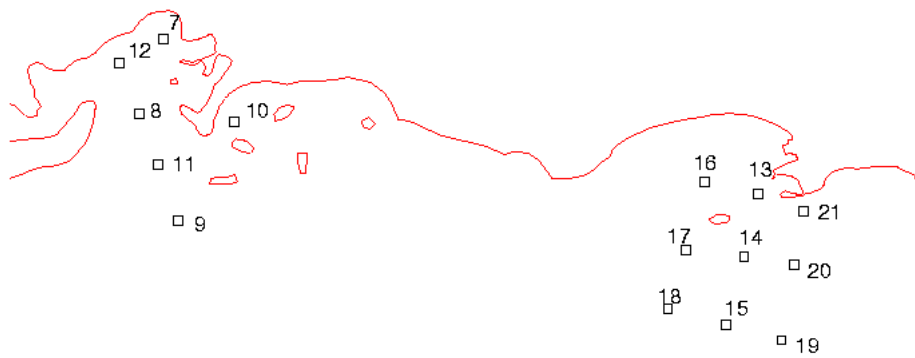


Figure 13 Reference stations for Ponce and Guayanilla

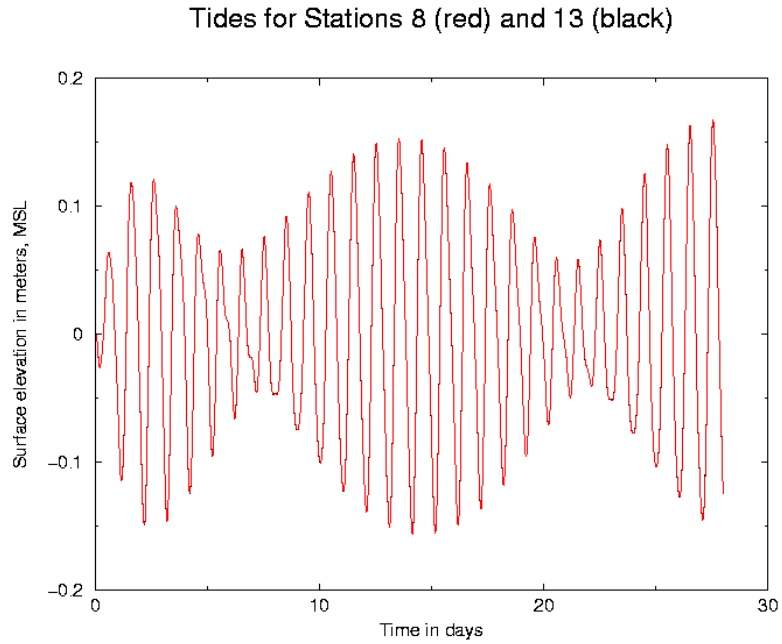


Figure 14 28-day tidal elevation time series for Station 8 and 13

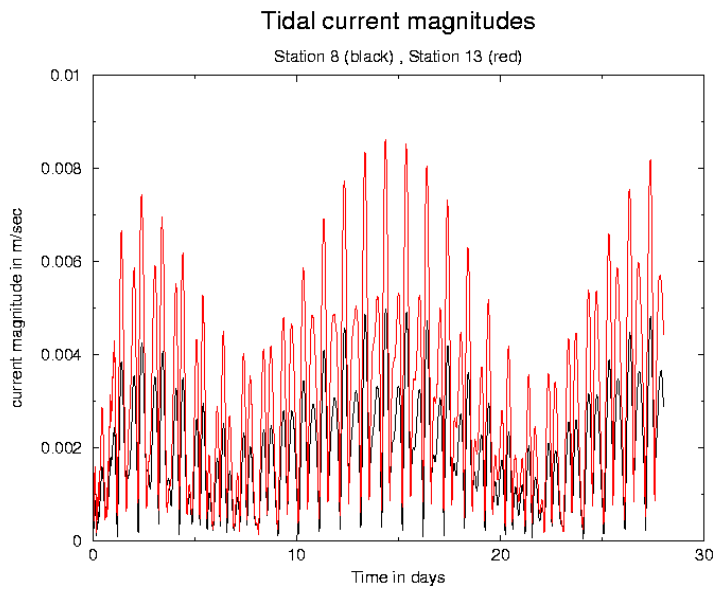


Figure 15 28-day tidal current magnitude pre-construction time series for Station 8 and 13

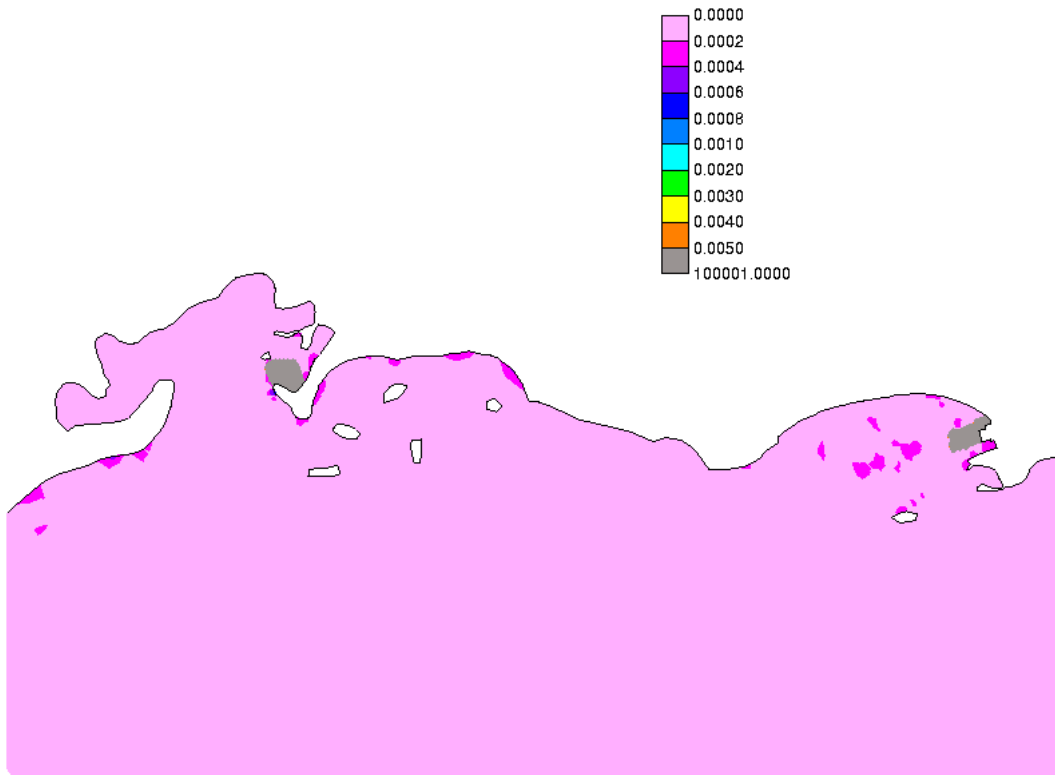


Figure 16 Maximum tidal elevations differences during days 12.5-17.5

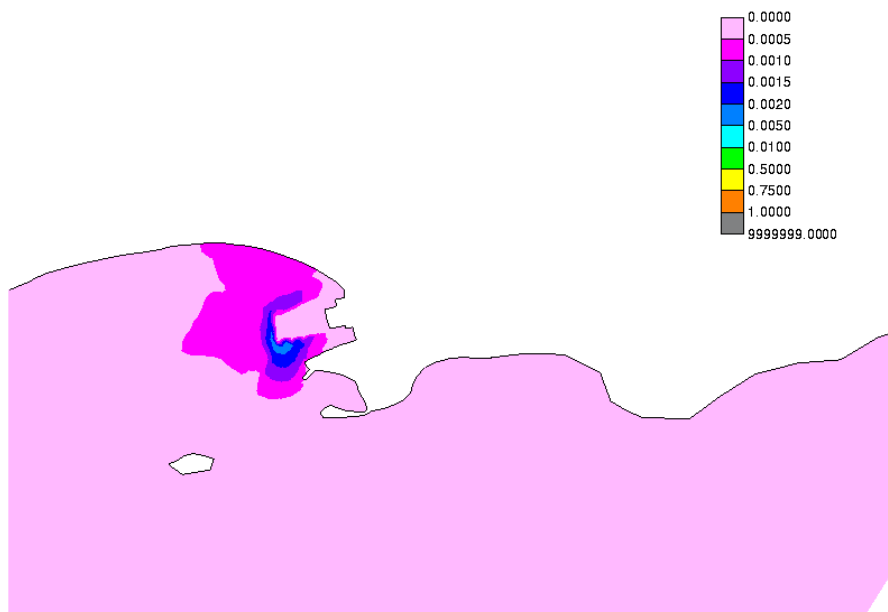


Figure 17 Maximum tidal current differences during days 12.5-17.5 for Ponce

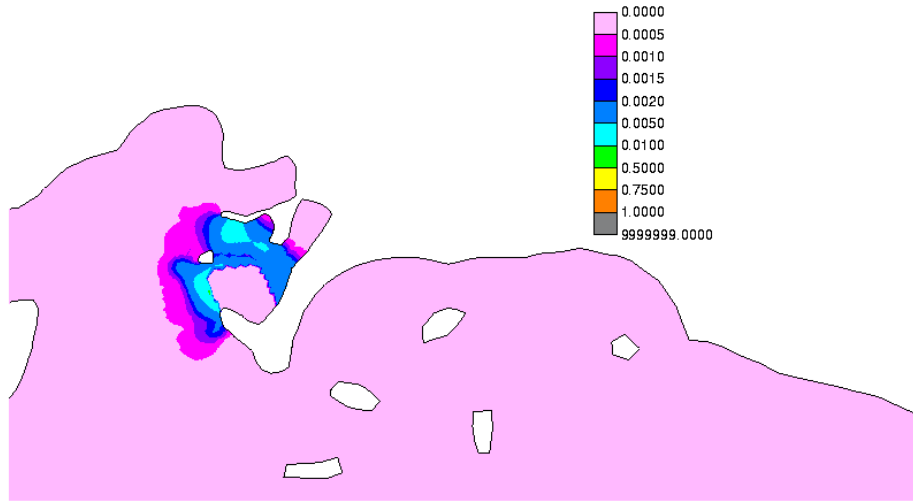


Figure 18 Maximum tidal current differences during days 12.5-17.5 for Guayanilla

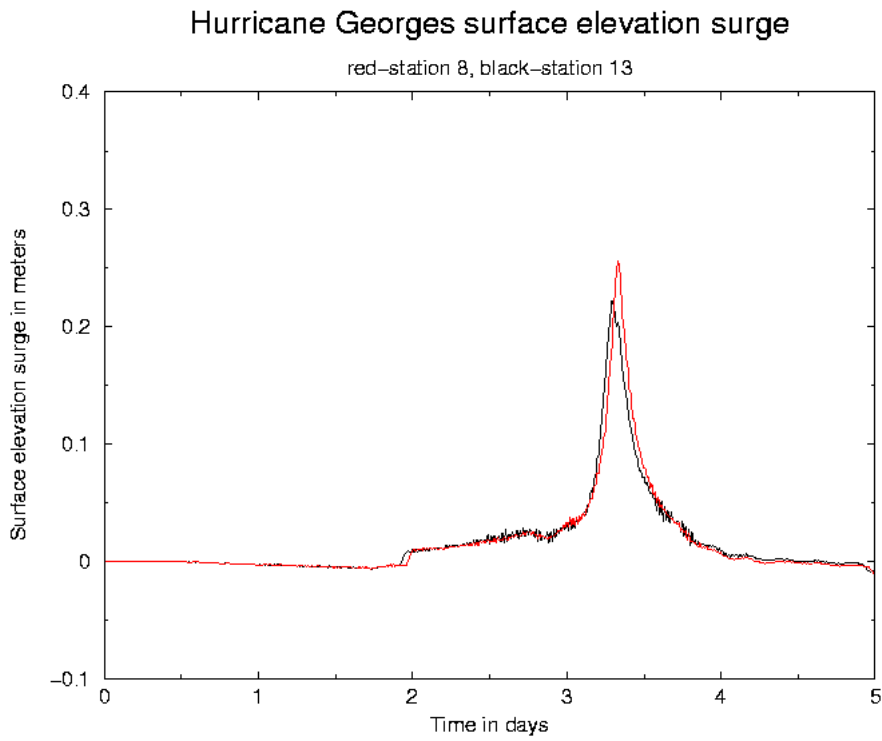


Figure 19 Storm surge elevation for Hurricane Georges at Stations 8 and 13

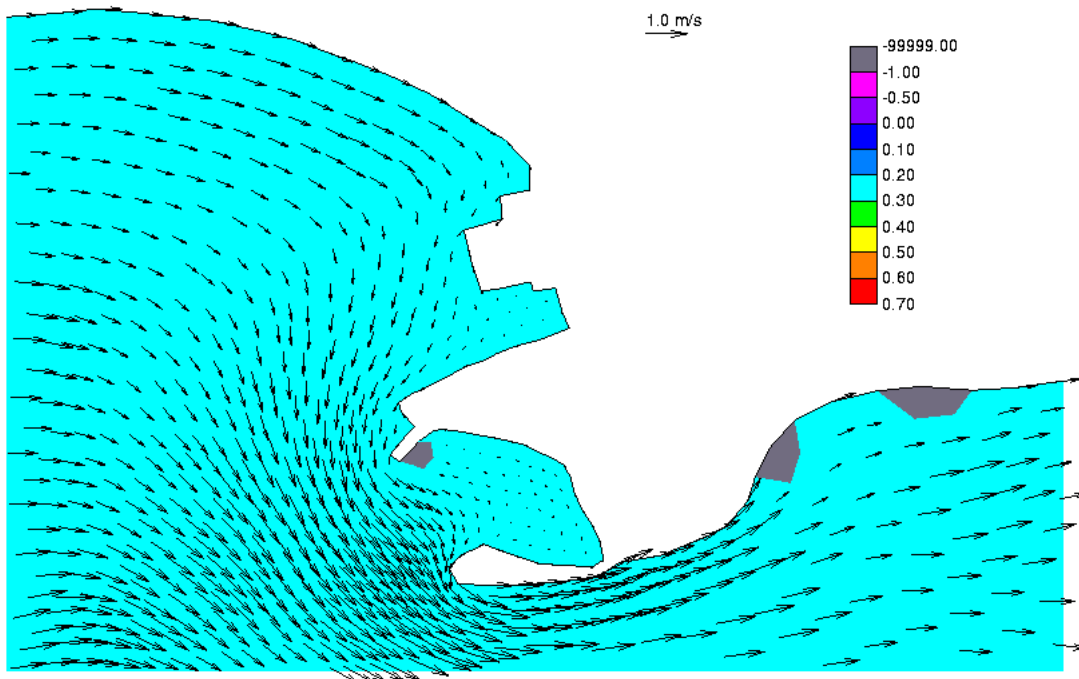


Figure 20 Pre-expansion circulation vectors at Ponce for Hurricane Georges at day 3.28

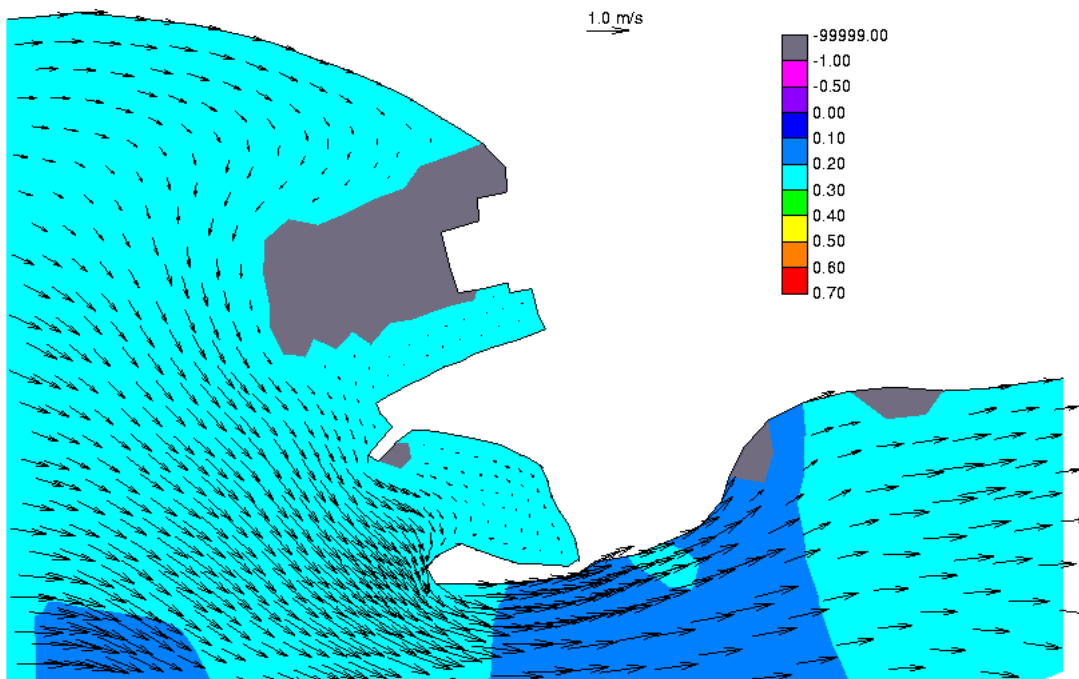


Figure 21 Post-expansion circulation vectors at Ponce for Hurricane Georges at day 3.28

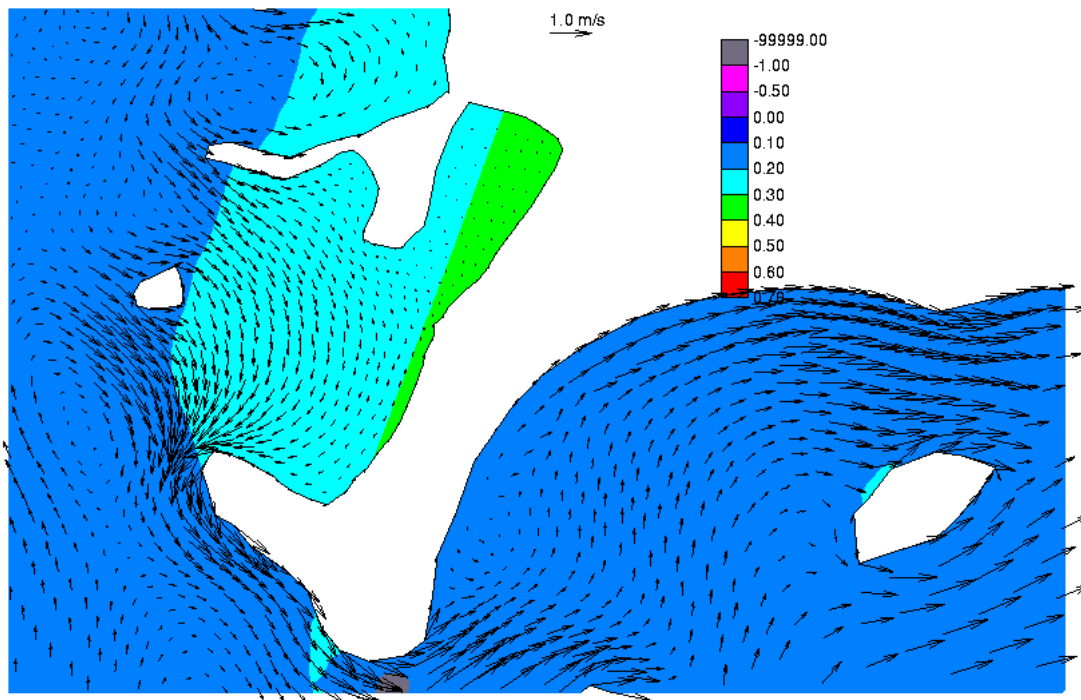


Figure 22 Pre-expansion circulation vectors at Guayanilla for Hurricane Georges at day 3.28

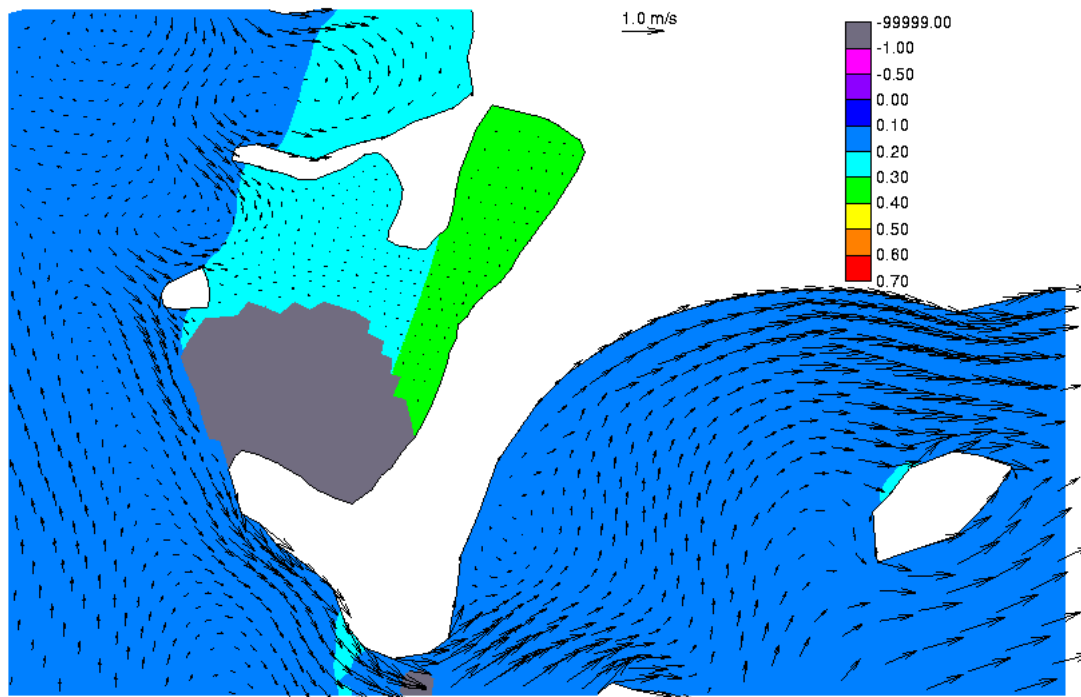


Figure 23 Post-expansion circulation vectors at Guayanilla for Hurricane Georges at day 3.28

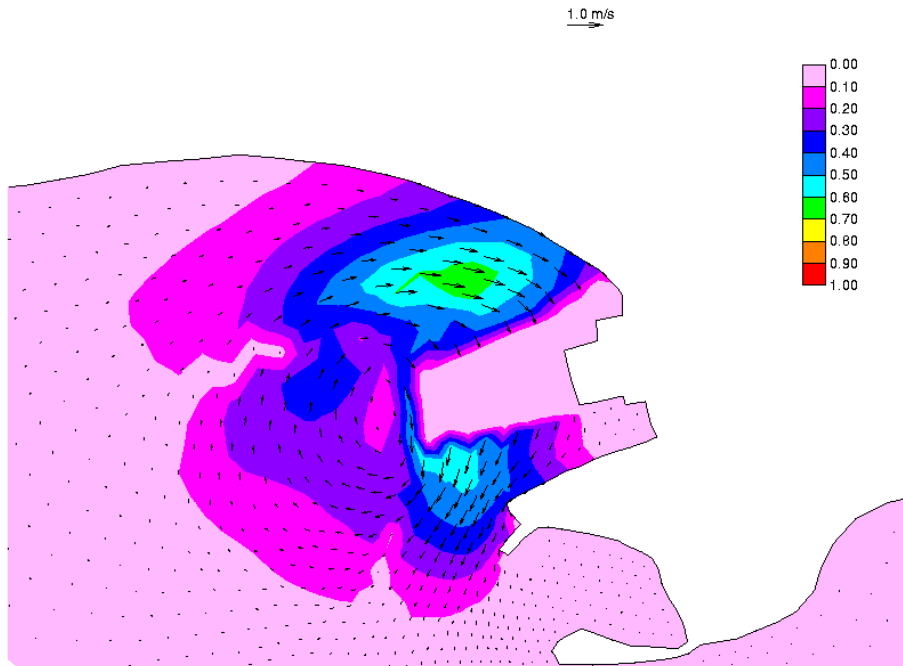


Figure 24 Maximum current difference at Ponce for Hurricane Georges

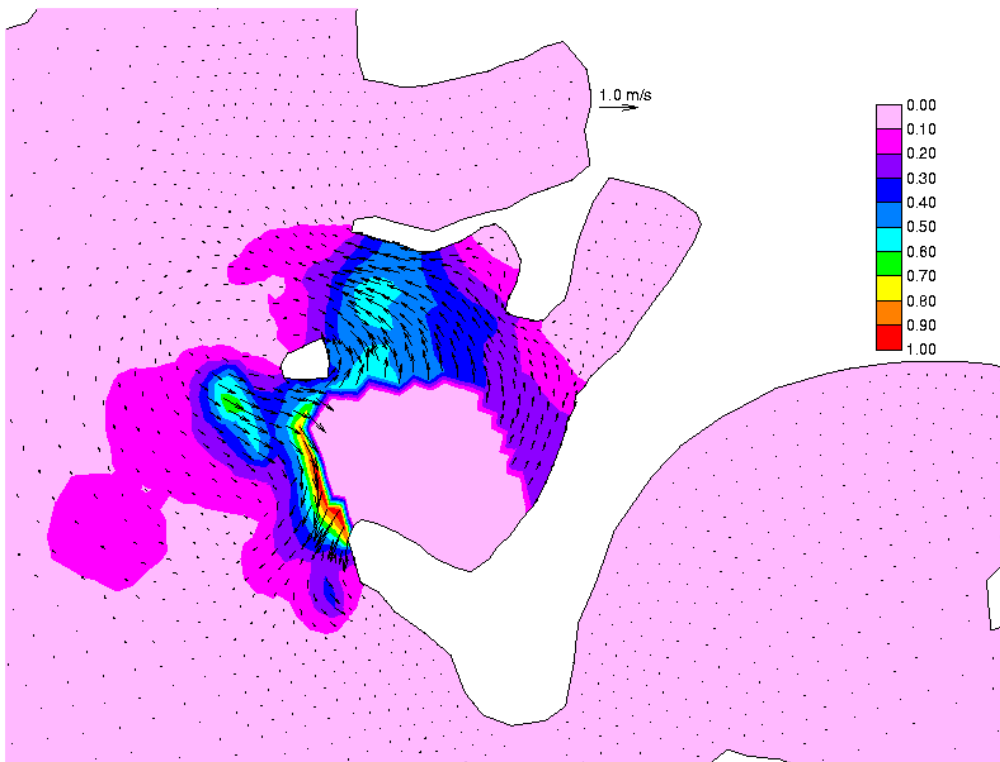


Figure 25 Maximum current difference at Guayanilla for Hurricane Georges

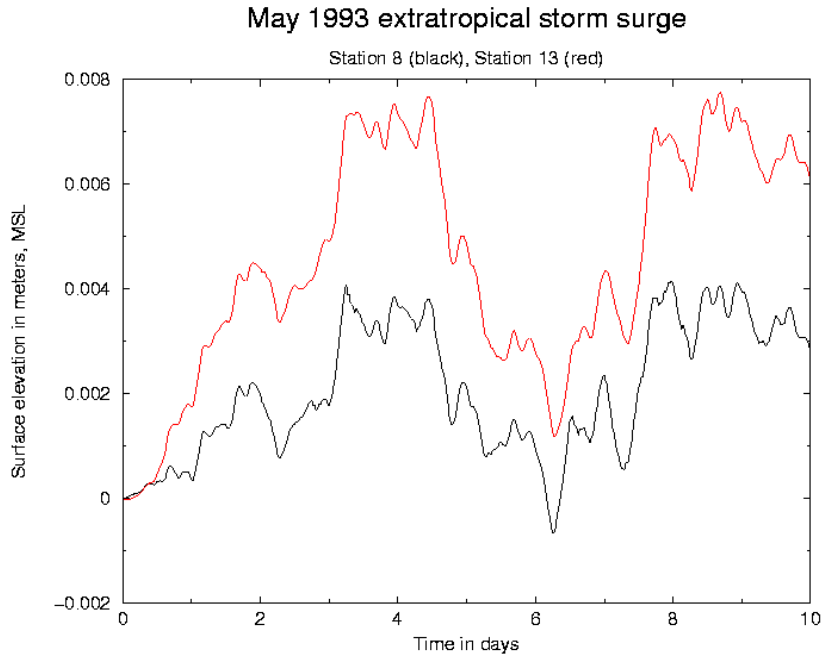


Figure 26 Extratropical storm surge elevation at day 8.125 at Stations 8 and 13

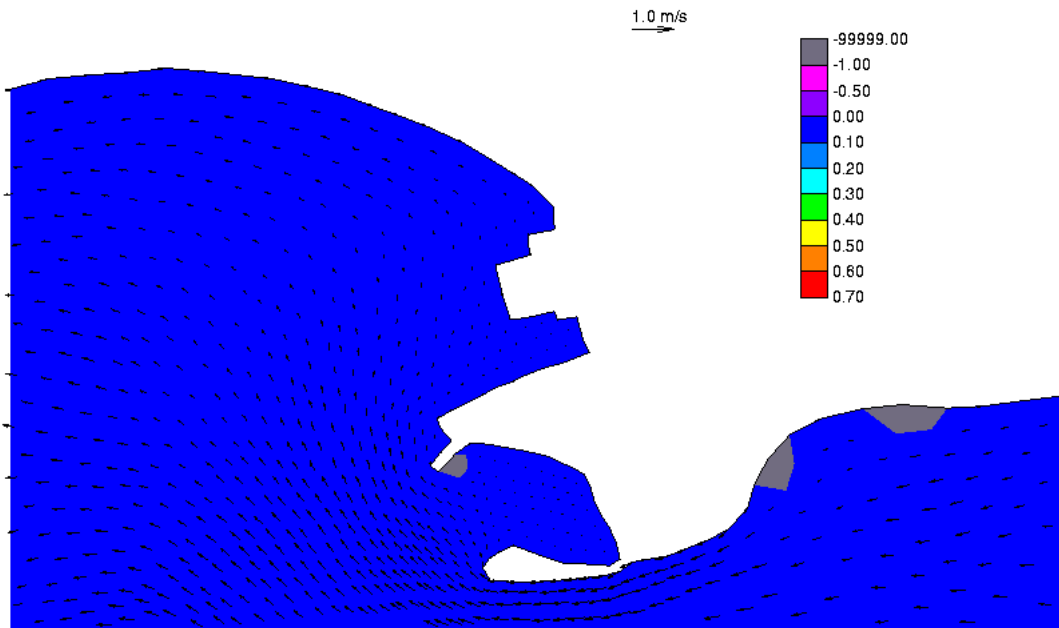


Figure 27 Existing condition extratropical storm circulation vectors at Ponce at day 8.125

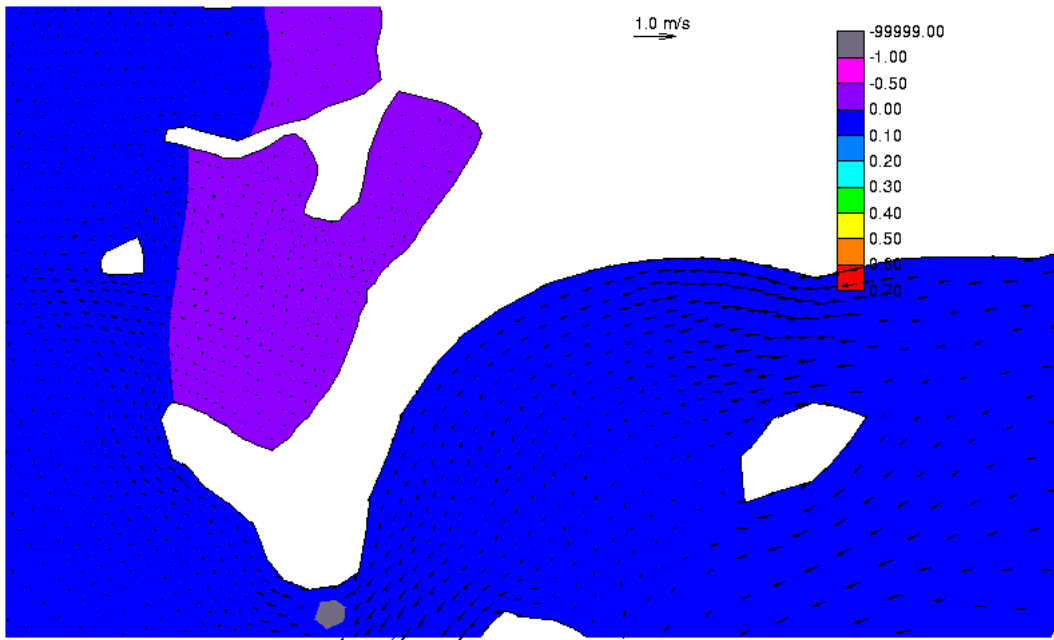


Figure 28 Existing condition extratropical storm circulation vectors at Guayanilla at day 8.125

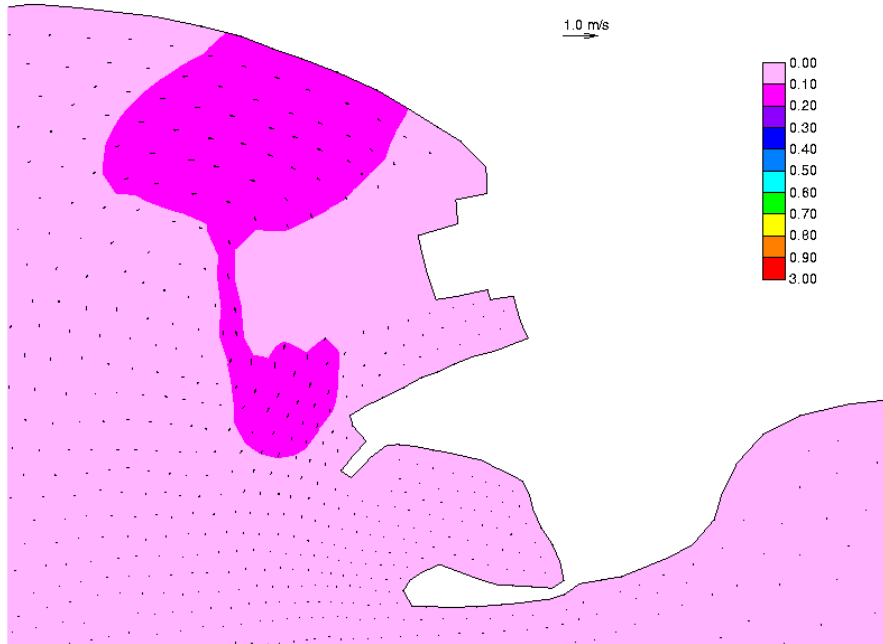


Figure 29 Maximum extratropical current difference at Ponce

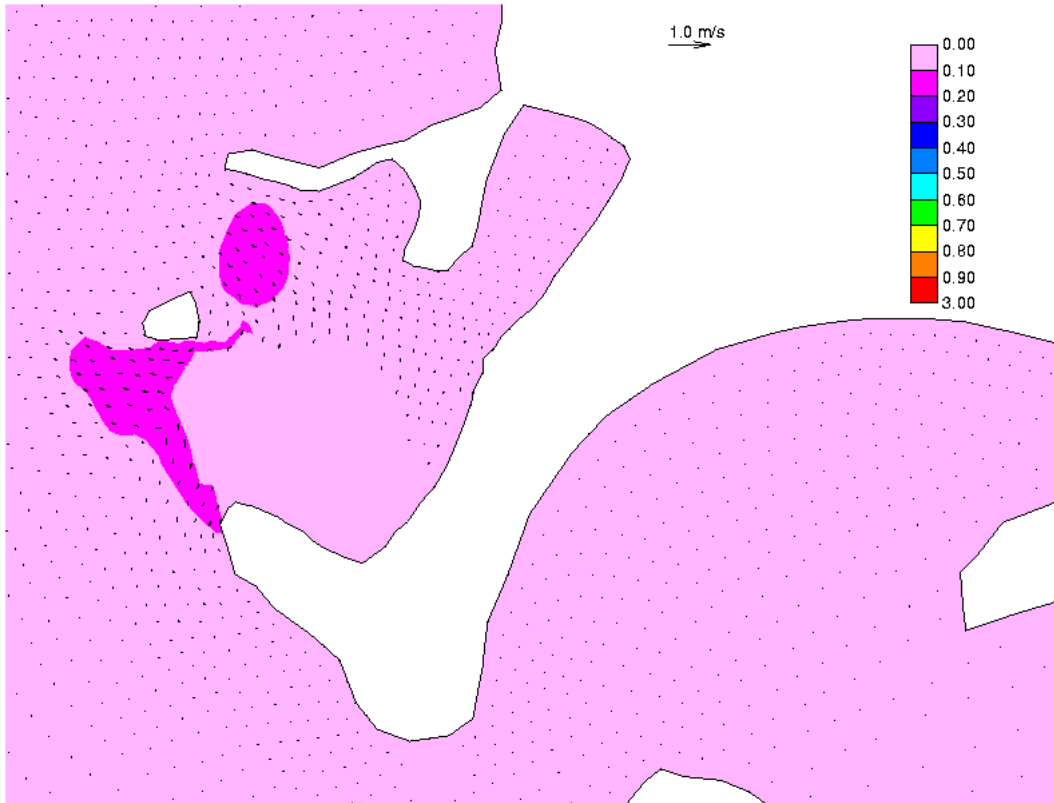


Figure 30 Maximum extratropical current difference at Guayanilla

APPENDIX A: TIDAL VERIFICATION

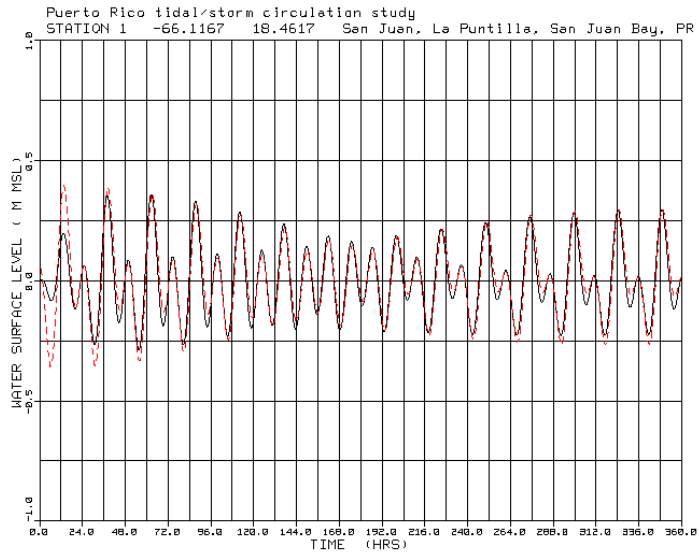


Figure 1A Station #1, San Juan, La Puntilla, San Juan Bay, PR

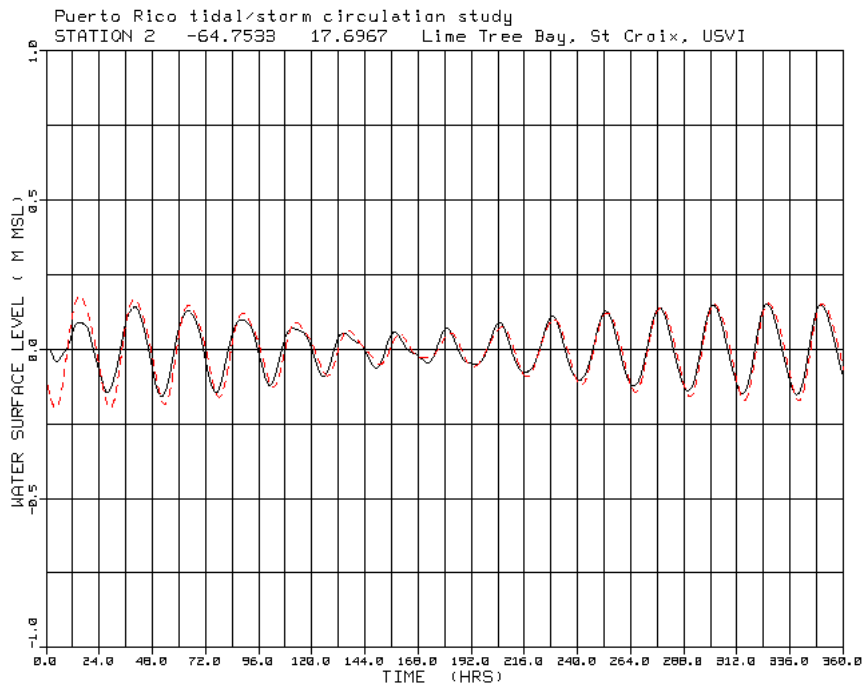


Figure 2A Station #2, Lime Tree Bay, St Croix, USVI

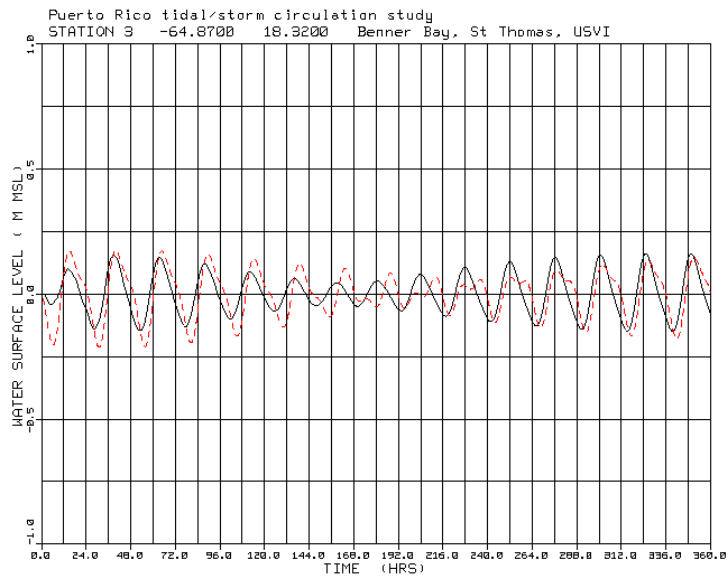


Figure 3A Station #3, Benner Bay, St Thomas, USVI

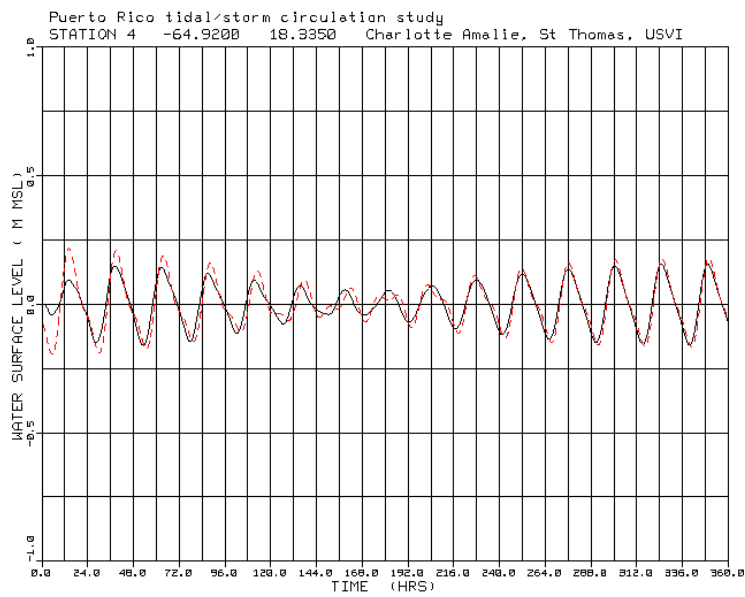


Figure 4A Station #4, Charlotte Amalie, St Thomas, USVI

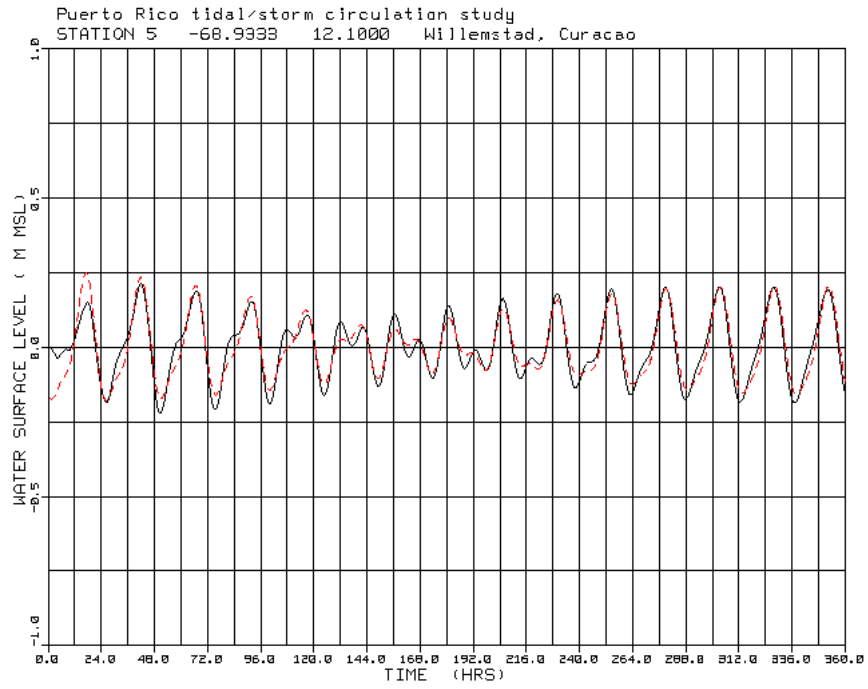


Figure 5A Station #5, Willamstat, Curacao

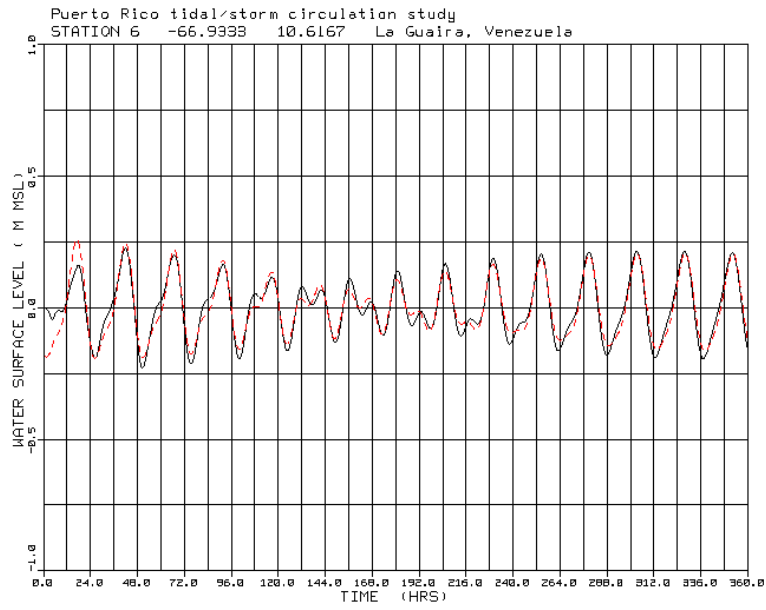


Figure 6A Station #6, La Guaira, Venezuela

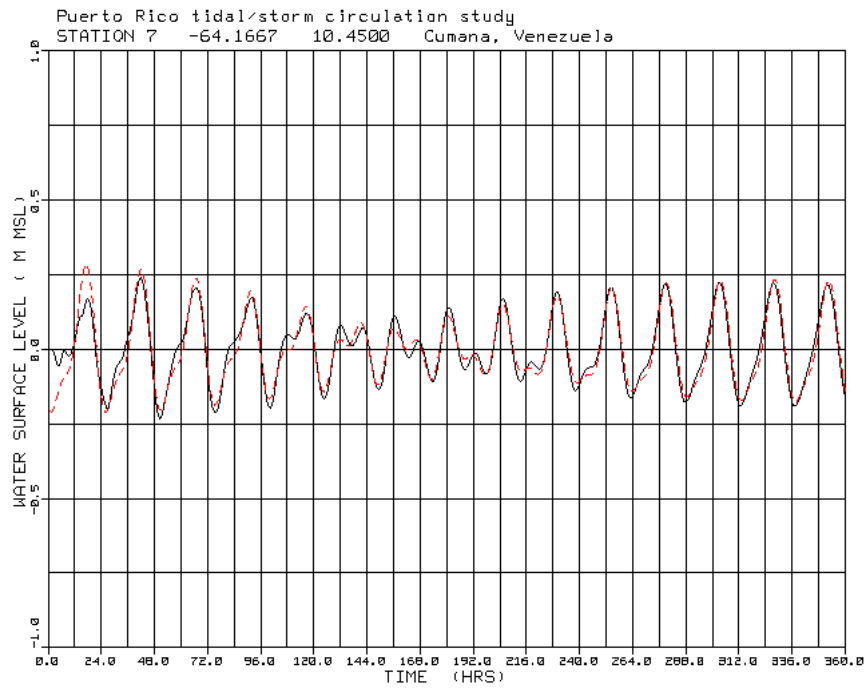


Figure 7A Station #7, Cumana, Venezuela

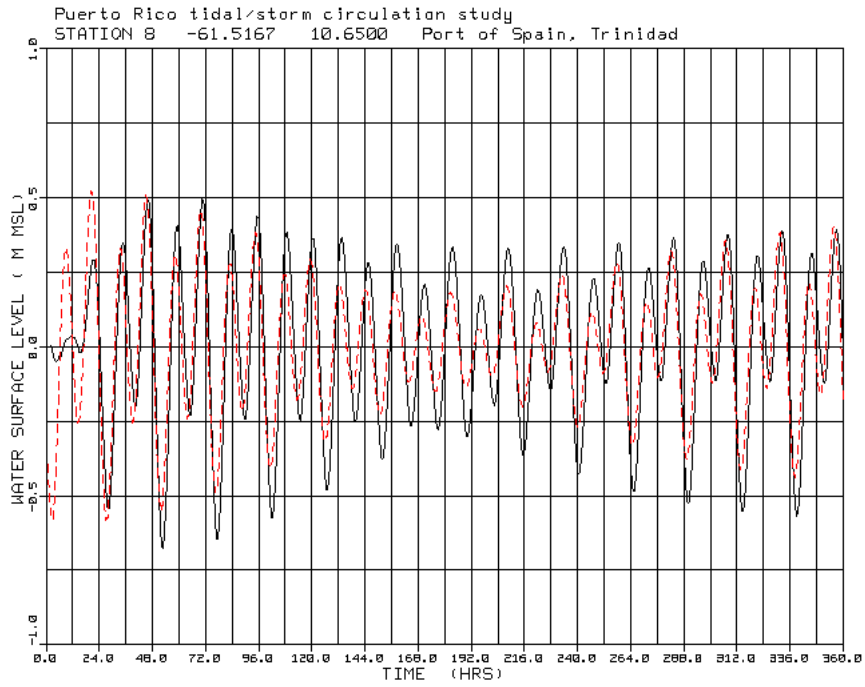


Figure 8A Station #8, Port of Spain, Trinidad

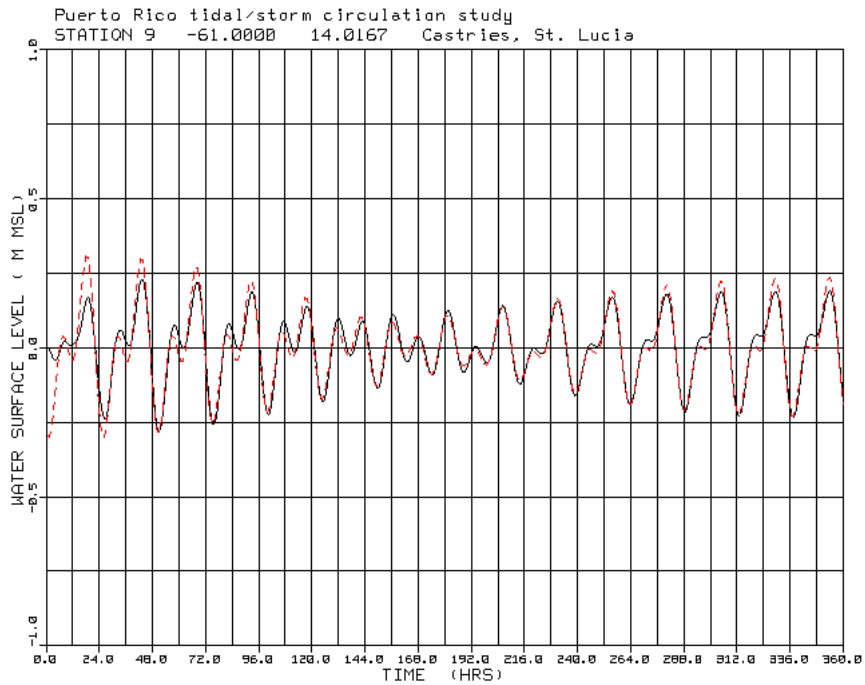


Figure 9A Station #9, Castries, St. Lucia

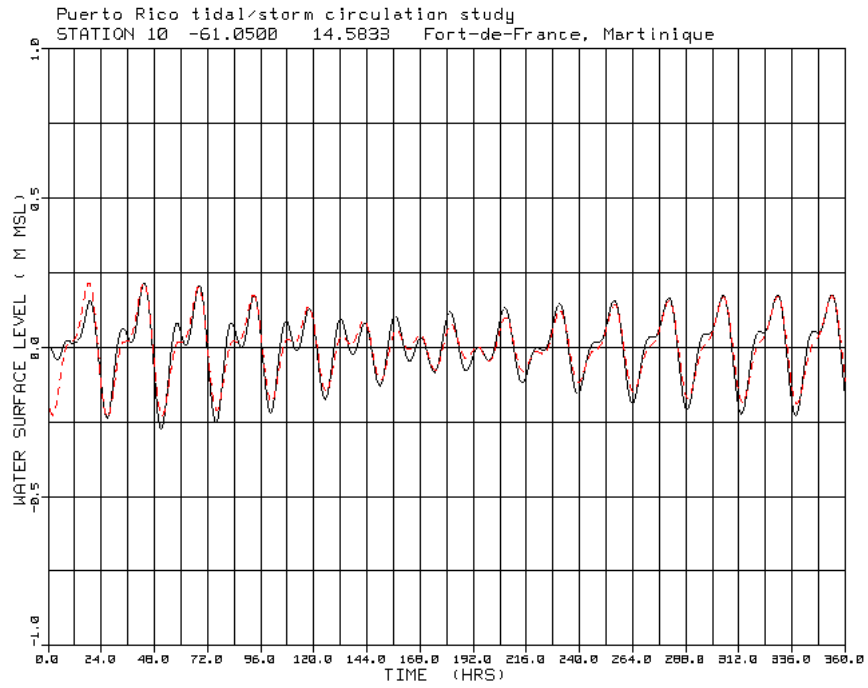


Figure 10A Station #10, Fort-de-France, Martinique

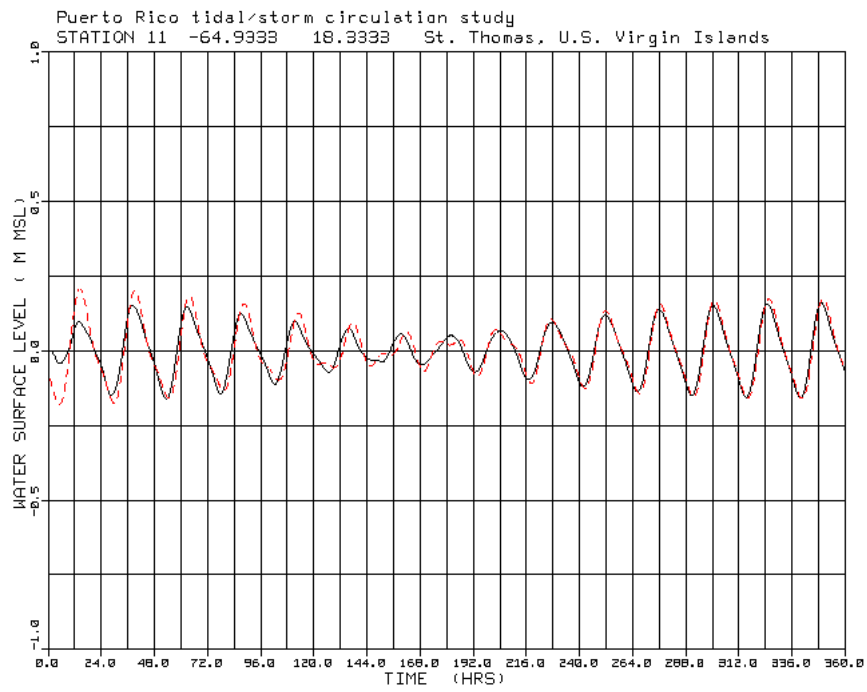


Figure 11A Station #11, St. Thomas, U.S. Virgin Islands

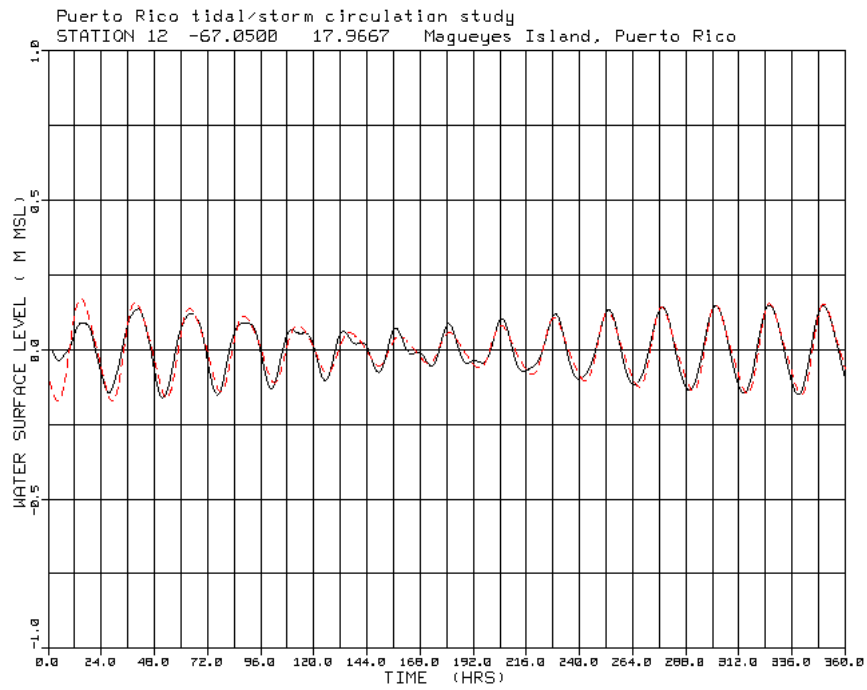


Figure 12A Station #12, Magueyes Island, Puerto Rico

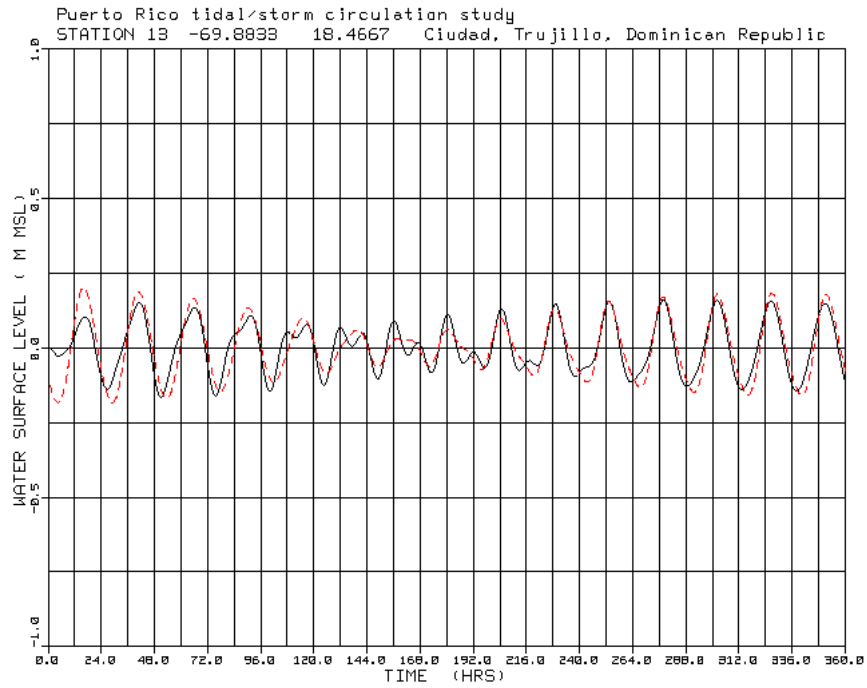


Figure 13A Station #13, Ciudad, Trujillo, Dominican Republic

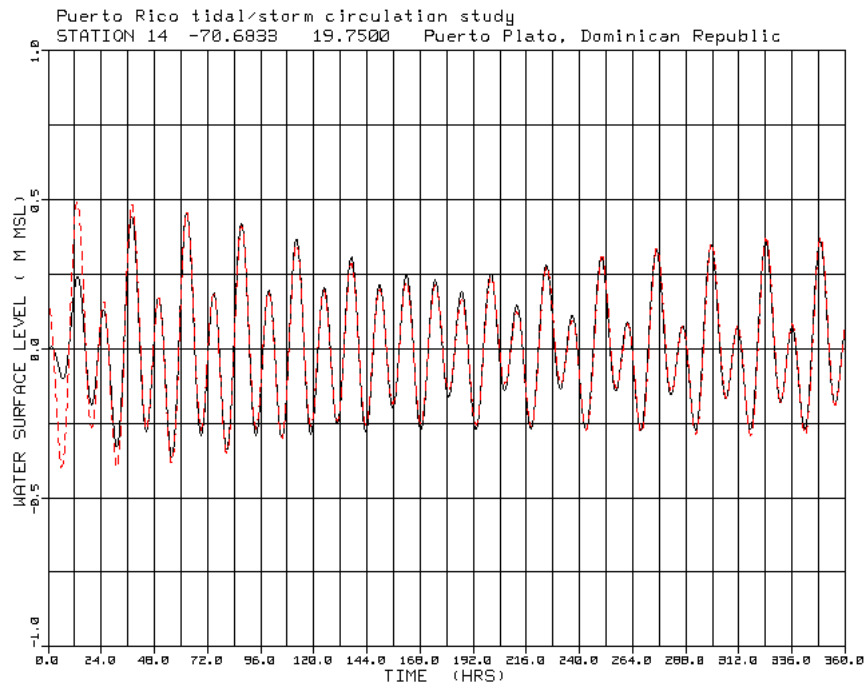


Figure 14A Station #14, Puerto Plato, Dominican Republic

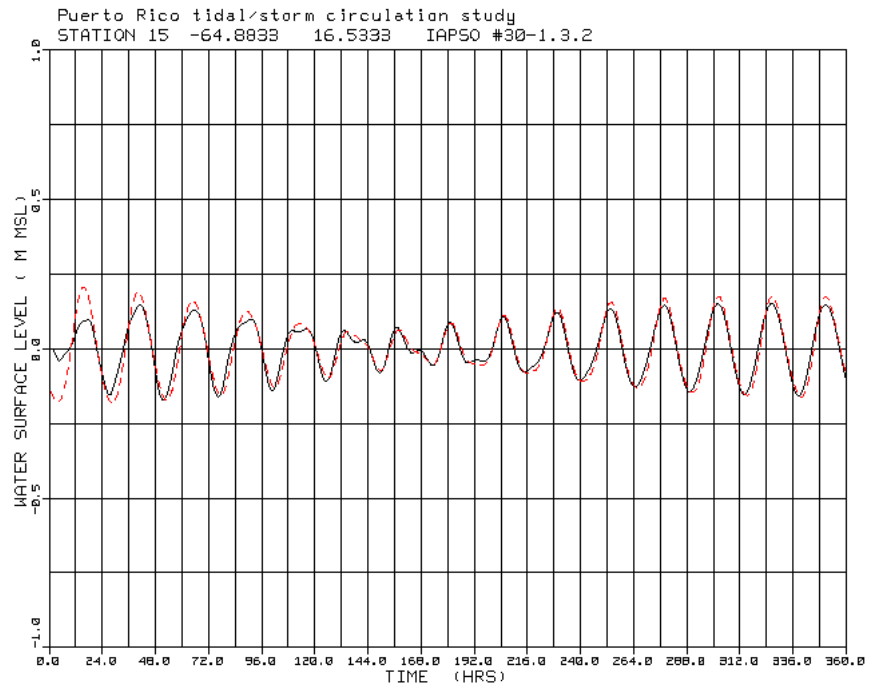


Figure 15A Station #15, IAPSO #30-1.3.2